UNIVERSIDADE D
COIMBRA

Sara Maria Santos Soares Dias

THERMAL AND MECHANICAL BEHAVIOUR OF SANDWICH PANELS FOR CLIMATIC CHAMBERS OF HIGH PERFORMANCE

VOLUME 1

Dissertação no âmbito do Mestrado em Engenharia de Materiais orientada pelo Professor Doutor Amílcar Lopes Ramalho e pelo Professor Doutor António José Barreto Tadeu e apresentada ao Departamento de Engenharia Mecânica

Julho de 2020

1 2 9 0

FACULDADE DE CIÊNCIAS E TECNOLOGIA
UNIVERSIDADE D COIMBRA

Caracterização do comportamento térmico e mecânico de painéis sandwich para câmaras climáticas de elevada performance

Dissertação apresentada para a obtenção do grau de Mestre em Engenharia de Materiais

Thermal and mechanical behaviour of sandwich panels for climatic chambers of high performance

Autor

Sara Maria Santos Soares Dias

Orientadores

Professor Doutor Amílcar Lopes Ramalho

Professor Doutor António José Barreto Tadeu

Colaboração Institucional

itecons

Itecons - Instituto de Investigação e Desenvolvimento Tecnológico para a Construção, Energia, Ambiente e Sustentabilidade

Coimbra, julho, 2020

Success consists of going from failure to failure without loss of enthusiasm

Winston Churchill

Acknowledgments

I would like to start by thanking to my thesis supervisors, Professors António Tadeu and Amilcar Ramalho.

Professor Tadeu, I would like to thank him to be such an enthusiastic of scientific work and responsible for passing that enthusiasm to so many people around him including myself. Professor Tadeu teach me to never give up, to seek the reasons of failure, to structure and express ideas, to physically criticize and understand results, etc. He helped me to have in mind the big picture that I sometimes could not see.

To Professor Amilcar, I would like to thank him for sharing his huge experience with me, practical and theoretical. I also would like to thank him for the patience in the lab.

More than an individual work, this thesis is the result of the combined efforts. Having that in mind I would like to show my acknowledgment and appreciation for all of those who have helped me, starting to my colleagues of work which I can also call friends: Filipe Pedro, Tiago Jesus and Michael Brett. I would like to thank them for the patience that they showed in the countless times of test rig preparation, and for their knowledge and friendship. In the case of Michael, I would also to thank him for the huge help with English. I am sincerely grateful for all you already teach me and for what I believe I improve thanks to him. In the end of this journey I had the luck of having another English language specialist, Catarina Serra, which I would like to sincerely thank. I would like to thank to Katya Coelho, who helped me with thermal conductivity tests.

I would also like to present and institutional acknowledgments to Itecons and to co-promotion project, NewGenShell – New Generation High Performance Shells for Climatic Chambers (POCI-01-0247-FEDER-033413 / LISBOA-01-0247-FEDER-033413).

My deepest gratitude goes to my family, for everything. To my parents who gave me the tools and to my little sister that despite of the young age is an example in so many ways.

Abstract

Climate chamber tests are becoming more prevalent as the quality level expected from products and components increases. As testing conditions become more demanding, the elements that make up the envelope of the chambers, usually sandwich panels, are exposed to a wide range of temperatures. It is important to understand how the mechanical and thermal properties of the core materials in the sandwich panels change when subjected to these temperatures.

In this context, this work was set out to perform a thermal and mechanical characterisation of four core materials often used in sandwich panels: balsa wood, mineral wool (MW), and polyethylene terephthalate (PET), polyurethane (PUR) rigid foams.

The thermal characterisation focused on two main thermal properties: thermal conductivity and specific heat. To evaluate these features, an experimental setup was developed to reflect a real application scenario. In it, one of the surfaces of the sandwich panels is submitted to a high temperature, while the other faces the indoor room temperature, creating a thermal gradient that generates heat transfer between both environments. The setup allowed the study of thermal behaviour for different temperature levels. Each test comprised of 5 temperature steps: 40ºC, 80ºC, 120ºC, 160ºC, and 200ºC. The test procedure included steady state (for predefined temperature levels) and unsteady state periods, resulting from the temperature level transition. This made it possible to determine the effect of temperature on thermal conductivity and specific heat. It was also possible to observe the effect of temperature on the materials' appearance and structural integrity. Thermal conductivity at 10^{o}C was also experimentally determined in accordance with normalized methodologies and equipment. These results were in accordance with the thermal conductivity determined for the first temperature level, validating the developed experimental setup. Regarding specific heat capacity, an indirect method was used. This method combines the experimental data with results from a one-dimensional analytical transient heat transfer model, by aligning the experimental values registered by thermocouples with the analytical results using an iterative approach.

Regarding the mechanical characterisation the feasibility of using impulse excitation technique (IET) to evaluate the variation of Young's modulus of these materials with temperature was evaluated. The polymeric foams were studied up to 100 ºC, balsa wood was studied up to 160 ºC, while mineral wool was excluded from this test. This study was validated with static four-point bending tests. The application of this technique eliminates the need to perform static tests in which universal testing machines are placed inside climatic chambers. Additionally, other mechanical tests were performed: shear tests to determine shear resistance, four-point-bending tests in order to understand how shear contributes for rupture in bending, and compression tests to determine compression resistance. All of these tests were carried out at room temperature.

Keywords: Sandwich panel, Mechanical behaviour, Thermal behaviour, thermal conductivity, specific heat, elastic modulus, Young's modulus, climatic chambers

Resumo

Os testes realizados em câmaras climáticas são cada vez mais comuns à medida que o nível de qualidade esperado dos produtos e componentes aumenta. Ao passo que as condições de testes se tornam mais exigentes, os elementos que compõem o invólucro das câmaras, geralmente painéis sanduíche, são expostos a uma ampla gama de temperaturas. É importante entender como as propriedades mecânicas e térmicas dos materiais do núcleo nos painéis sanduíche mudam quando submetidas a essas temperaturas.

Nesse contexto, este trabalho teve como objetivo realizar uma caracterização térmica e mecânica a quatro materiais frequentemente utilizados em núcleos de painéis sanduíche: balsa, lã mineral, espumas rígidas tereftalato de polietileno (PET), e de poliuretano (PUR).

A caracterização térmica focou-se em duas propriedades térmicas principais: condutividade térmica e calor específico. Para avaliar estas propriedades, foi desenvolvida uma configuração experimental que refletisse um cenário de aplicação real. Uma das superfícies dos painéis sanduíche é submetida a alta temperatura, enquanto a outra fica a temperatura ambiente, criando um gradiente térmico que gera transferência de calor entre os dois ambientes.

Esta configuração permitiu o estudo do comportamento térmico para diferentes níveis de temperatura. Cada teste consistiu em 5 etapas de temperatura: 40ºC, 80ºC, 120ºC, 160ºC e 200ºC. O procedimento de teste incluiu períodos de regime permanente (para níveis de temperatura predefinidos) e períodos de regime transiente, resultantes da transição do patamar de temperatura. Assim, foi possível determinar o efeito da temperatura na condutividade térmica e no calor específico. Também foi possível observar o efeito da temperatura na aparência e na integridade estrutural dos materiais. A condutividade térmica a 10ºC foi também determinada experimentalmente de acordo com metodologias e equipamentos normalizados. Estes resultados estavam de acordo com a condutividade térmica determinada para o primeiro nível de temperatura, validando a configuração experimental desenvolvida. Em relação ao calor específico, foi utilizado uma metodologia

indireta. Este método combina os dados experimentais com os resultados de um modelo de transferência de calor transitório analítico unidimensional, alinhando os valores experimentais registrados pelos termopares com os resultados analíticos usando uma abordagem iterativa.

Em relação à caracterização mecânica, foi avaliada a viabilidade do uso da técnica de excitação por impulso (IET) para avaliar a variação do módulo de Young destes materiais com a temperatura. As espumas poliméricas foram estudadas até 100 ºC, a balsa foi estudada até 160ºC, enquanto a lã mineral foi excluída deste teste. Este estudo foi validado com testes estáticos de flexão-quatro pontos. A aplicação desta técnica elimina a necessidade de realizar testes estáticos nos quais máquinas universais de ensaio são colocadas dentro de câmaras climáticas. Além disso, outros testes mecânicos foram realizados: testes de corte para determinar a resistência ao corte, testes de flexão-quatro pontos para perceber como o corte contribui para a rotura em flexão e testes de compressão para determinar a resistência à compressão. Todos estes testes foram realizados à temperatura ambiente.

Palavras-chave Painéis Sandwich, Comportamento mecânico, Comportamento térmico, condutibilidade térmica, calor específico, módulo de elasticidade, módulo de Young, câmaras climáticas.

Contents

LIST OF FIGURES

LIST OF TABLES

ACRONYMS

ASTM – American Society for Testing and Materials

CFC's - Chloro-Fluoro-Carbons

GFRP - Glass Fibre Reinforced Polymer

IET - Impulse Excitation Technique

MW – Mineral Wool

NewGenShell - New Generation High Performance Shells for Climatic Chambers (projet name)

PET - Polyethylene terephthalate

PUR - Polyurethane

PVC - Polyvinyl Chloride

RH - Relative Humidity

Tg - Glass-Transition Temperature

Tm - Melting temperature

1. INTRODUTION

1.1. Scope

High-performance and large-scale climatic chambers are usually sandwich solutions that operate under adverse service conditions. However, the construction of the "shells "of these chambers follows conventional manufacturing processes.

The insulation panels used are, mostly made from injected polyurethane have limited structural and thermal resistance, and are, not suitable to overcome big spams (large-scale) and to endure aggressive hygrothermal cycles (high-performance).

There are several important aspects that require further research studies for this kind of application. Namely there is a need for the design of more sustainable, more structurally resistant, and more energy efficient solutions, among others. In the context of designing and evaluating such solutions, there is a demand for accurate information about the materials. Usually, this kind of information (regarding thermal and mechanical behaviour) is only given for ambient conditions, which may be very different from the service conditions of this kind of application.

The mechanical behaviour of this type of construction (sandwich structures) has been studied over the years, especially regarding bending and shear. Nowadays, there is a bigger concern in understanding how the materials that compose the panels behave under the effect of temperature and temperature variation.

The service conditions of the climatic chambers do not only affect the mechanical behaviour but also have impact on thermal performance. The effect of temperature on thermal properties is often dismissed and the values used as reference do not take this effect into consideration. Service temperatures can be substantial (up to 180 ^{o}C, sometimes more) and under these conditions the thermal behaviour of some materials can be far below the expected.

1.2. Objectives and motivation

Climatic chambers have been used to test products for diverse applications, such as components for the automotive, aerospace, electronics, medical and consumer sectors, for over 100 years. However, the increasing demand regarding the level of quality of products has led to, more demanding tests and conditioning requirement.

In the context of the NewGenShell, a co-promotion project, (in partnership with the industry) a goal was set to develop climatic chamber envelopes which differ from the existing solutions, through the conception and design of envelopes for larger and more competitive modular chambers.

The objective is for these shells to efficiently respond to extreme operating conditions and to have less of an impact on the environment. The intended environment improvements will come from, not only using more sustainable materials, but also from the design being more efficient, as result of a deeper understanding of the materials' behaviour under service conditions.

In the scope of this Master's degree, the intent is to contribute to the development of sandwich panels that exhibit good mechanical and thermal behaviour, in extreme temperature conditions, have good mechanical and thermal behaviour. The experimental plan involves, the characterization of different properties (thermal and mechanical) of different core materials under different temperature conditions.

1.3. Document structure

This dissertation is divided into five chapters. First, the introduction, which includes the scope, the objectives and motivation for this work, and a brief presentation of the dissertation structure.

Secondly, the state of the art introduces the theme under study and provides a historical background on this subject, which is followed by a bibliographic research of scientific work published about sandwich constructions and their core materials. This research mainly focuses on the thermal and mechanical behaviour of the core materials and on their performance under different temperatures.

The third chapter is reserved for the thermal characterization. This characterization includes an experimental campaign, the purpose of which is to, on one hand determine how the thermal properties are affected by temperature, and on the other hand to understand how temperature varies along the wall's thickness. In order to address this, a testing apparatus was developed to allow the carrying out of a test with one of the specimens' surface at a defined temperature (simulating the interior of the climatic chamber) and the other at an external temperature (room temperature), thereby creating a thermal gradient similar to a real life application. In this chapter, the mewly developed experimental methodologies are presented and the main results are gathered. Also included is the theoretical approach which was the base for the determination of thermal parameters using experimental data.

The next chapter, dedicated to the mechanical characterization of the materials studied, presents the dynamic and static analysis techniques used. For each type of test performed, the objectives and principles of the tests are outlined. Finally, the results obtained are presented and discussed.

The last chapter is assigned to the conclusions of the thermal and mechanical characterisation, where the work is summarized.

2. STATE OF THE ART

2.1. Historical context

The concept of using sandwich construction elements was first discussed by Duleau, in 1820. However, this concept was only first applied commercially 100 years later (Zenkert, 1995).

As is commonly known, war conflicts demand scientific and technological development and sandwich constructions were part of this increase of knowledge. World War I saw the use of sandwich panels made from asbestos and a fibreboard core. In the 1930s, the appearance of structural adhesives allowed the creation of bonded sandwich composites, revolutionising the concept its application. World War II brought mass production of sandwich panels for the first time, using veneer faces with a balsa core (Zenkert, 1995).

The development of core materials soon followed, with the aim of reducing weight. Taking this into account, honeycomb core materials started to appear, promoted mainly by the aerospace industry. This solution offered the greatest shear strength and stiffness to weight ratios but required care in ensuring adequate bonding of the surfaces. However, the continued high cost of honeycomb cores has restricted their application predominantly to the aerospace and naval industries (in spite of their demands regarding resistance to corrosion).

Presently, different plastic materials are being used as the core material. In the early 1960s, polyvinyl chloride (PVC) and polyurethane (PUR) started to be used as core materials for medium cost applications. The possibility of producing cellular plastics with higher density solutions and greater rigidity opened this sandwich panel concept to a variety of new applications, namely in the construction, maritime and automotive industries and the in pre-fabrication of panels.

Sandwich constructions have been experiencing strong growth worldwide. The need for lightweight and high rigidity elements has increased the demand for this

construction technology, in particular for composite materials. The development of new production techniques has made it possible to produce sandwich panels at a more economical cost.

Today, the use of sandwich construction elements may be seen as a very common technology. However, this does not mean that it is not an important concept. On the contrary, each day it becomes more relevant, allowing quick, economic and efficient structural solutions. (Avó de Almeida, 2009).

2.2. Sandwich construction concept

A sandwich structure is defined by the American Society for Testing and Materials, as

a special form of a laminated composite comprising of a combination of different materials that are bonded to each other so as to utilise the properties of each separate component to the structural advantage of the whole assembly (Zenkert, 1995).

Usually sandwich constructions are made of at least three constituents, the face sheets, the core and the adhesive joints, see Figure 2.1.

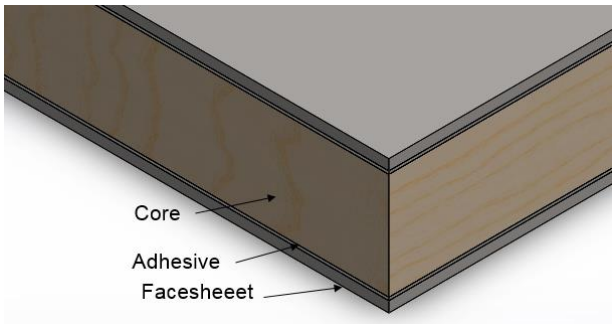

Figure 2.1. Sandwich panel constitution.

The concept of a sandwich structure is much the same as that of an I-beam, which is an efficient structural shape because the material is placed in the flanges situated farthest from the neutral axis, increasing the inertia and thus the resistant moment (Zenkert, 1995).

In a sandwich, the outer faces take the place of the flanges and the core takes the place of the web, (see Figure 2.2). The difference between them is that the core of a sandwich is of a different material from the faces and it provides a continuous support for the outer

faces rather than a concentrated narrow web. The core resists to shear and stabilises the faces against buckling or wrinkling. The bond between the outer faces and the core must be strong enough to resist the shear and tensile stresses that occur between them. Additionally, compressive strength of the core is also important, particularly when using lightweight, thin laminate skins, so as to prevent the thin skins from wrinkling, and failing in a buckling mode.

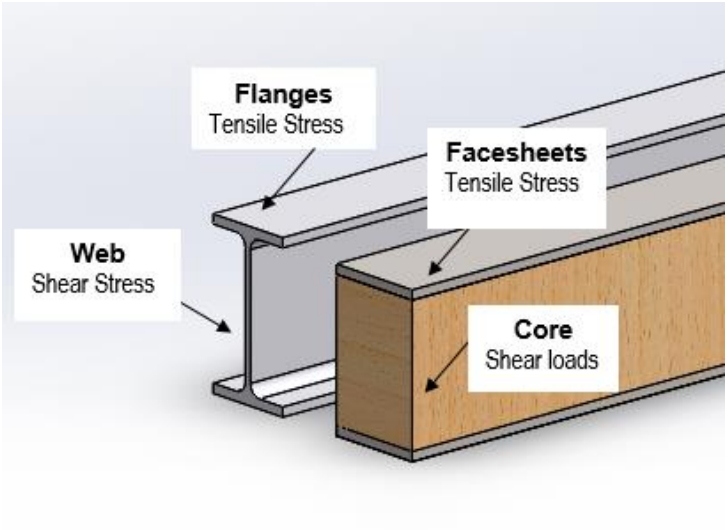

Figure 2.2. Structural parallelism between an I beam and sandwich panels (adapted from Davies, 2001).

The stress distributions in a structural sandwich construction can be simplified: the faces carry bending moments, such as tensile and compressive stresses, and the core carries transverse forces, such as shear stresses. This simplification is only possible because the elastic modulus of the face's material, Ef, is far greater than the elastic modulus of the core material, Ec. Furthermore, the thickness of the outer faces, tf, is much less than the core's thickness, tc. As these relations increase, the error of considering the stress distributions as illustrated in Figure 2.3.c) will reduce.

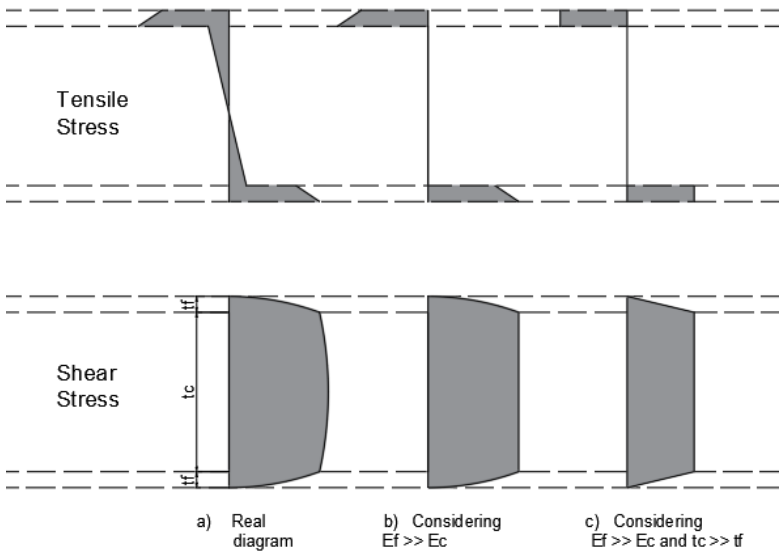

Figure 2.3. Tensile and shear stresses representation at the core and outer faces of a sandwich construction (adapted from Zenkert, 1995).

Sandwich construction is extremely structurally efficient, particularly in applications where stiffness is critical. The flexural stiffness, EI, for the same material, and therefore the same elastic modulus, E, is dictated only by the inertia moment, I. This parameter depends only on the geometry.

Considering a rectangular section with width b and thickness 2t, and a sandwich construction with the same width b, and with two faces with thickness t (set apart from each other at a distance c, corresponding to the core's thickness), the resulting equation for I is shown in Figure 2.4. It was assumed that only the faces are resisting. For the same area of resistant material, b ×2t, (disregarding the core material), the inertia moment is much larger for a sandwich construction than for an equivalent rectangular section.

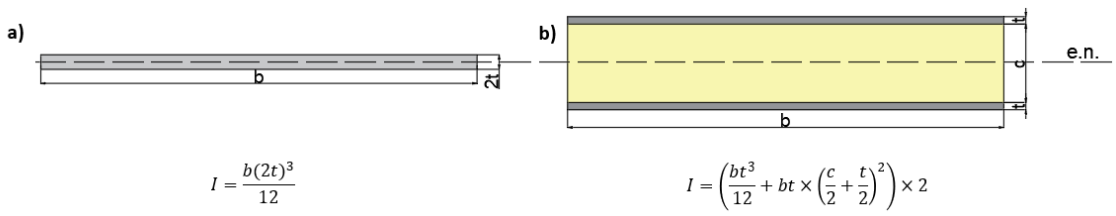

Figure 2.4. Relation between inertia moments: a) Rectangular section; b) Sandwich construction element section.

This explains why sandwich constructions are so efficient in terms of flexural strength. The section is more optimised as the material is positioned at a greater distance from the neutral axis. In the exercise shown in Figure 2.4, the neutral axis was considered to be positioned at middle of the sections. This is not always true, since the different sections that compose the sandwich panel may not be symmetrical.

The efficiency of these panels in terms of weight should also be taken into account. The face materials are much more resistant and consequently denser and heavier when compared with typical core materials. This means that the sandwich shown in Figure 2.4b) is stiffer than the rectangular section (Figure 2.4a), almost without increasing its overall weight.

2.3. Core materials

Under a mechanical point of view, the core must be able to resist to the applied transverse load and thus have a shear modulus high enough to guarantee the required shear stiffness.

However, core materials are often chosen on grounds that are not purely mechanical but rather for reasons related with resistance to weather, thermal insulation, the use of a specific manufacturing method, cost, wear resistance, sustainability, etc. These features depend essentially on the application and intended functionality of the panels.

Two sets of sandwich panels can be distinguished according to the following two groups of core materials: (i) homogeneous cores and (ii) non-homogeneous or structured cores, see Figure 2.5.

Non-homogeneous cores include ribbed cores, honeycomb cores and panels, where the face sheets are only point supported elements. Core materials of this type have been developed and used primarily in aerospace applications. However, cheap honeycomb materials made from impregnated paper are also used in building applications. The development of high density and high-quality cellular foams has had a major impact on the use of the sandwich concept. Homogeneous cores do not offer the same high stiffness and strength-to-weight ratios as honeycombs, but have other very important advantages. Namely, mostly they are less expensive than honeycombs but, more importantly, the manufacturing

of sandwich elements is easier and bonding is generally more efficient. In addition to this, homogeneous cores offer higher thermal insulation and higher corrosion resistance.

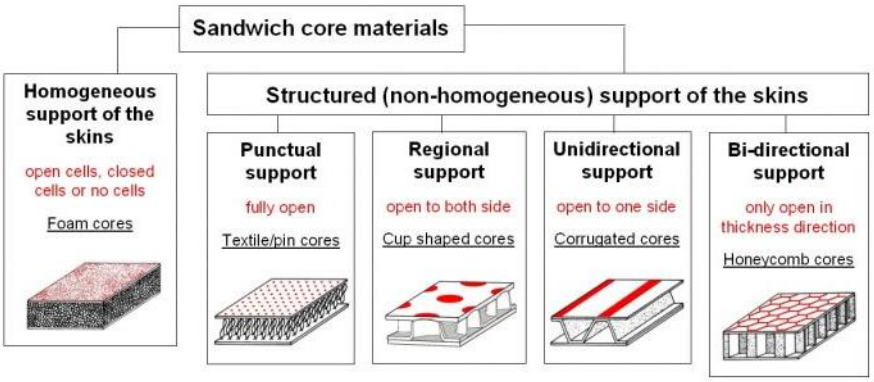

Figure 2.5: Representation of the principal cores used in load carrying sandwich constructions (Econcore, 2020).

In the present work, only homogeneous cores were used. The next sub-sections present some description and bibliographic research of the materials that are the base of the current study, polyethylene terephthalate (PET) foam, polyurethane (PUR) foam, balsa wood, and mineral wool (MW), shown in Figure 2.6.

a) b) c) d)

Figure 2.6. Materials studied: a) PET foam; b) PUR foam; c) Balsa wood; d) Mineral wool.

2.3.1. Polymer foams

Polymer foams are widely used because they have a lot of beneficial characteristics. When compared with other options, polymer foams present a substantial weight reduction because of its low density. The low density can be explained with their own production process. The polymer foams result from the fast combination of two phases, a solid and a gas phase. The gas that is used in the foam is known as blowing agent, and can

either be chemical or physical (Sivertsen, 2007). Chemical blowing agents are chemicals that take part in a reaction or that decompose, releasing substances in the process. Physical blowing agents are gases that do not react chemically in the foaming process and are therefore inert to the polymer forming the matrix (Sivertsen, 2007). The resulting foam has a polymer matrix with either air bubbles or air tunnels incorporated in it, which is known as either closed-cell or open-cell structure. Closed-cell foams are generally more rigid, while open-cell foams are usually more flexible (Sivertsen, 2007).

Since the gas has the least mechanical strength (the more gas there is, the less resistant the foam will be), lower density foams exhibit the smallest Young's modulus. Even if the cells of the foam have varying shapes, there is usually some anisotropy because of the direction of the foam being formed. The geometry of the cells could have more to say for the strength than density, chemistry and the amount of open-cells in the structure (Sivertsen, 2007). Moreover, it is also possible to vary the material's structure within a single group of foams by changing the detailed recipe or manufacturing process. (Davies, 2001)

The materials that provide the most of thermal insulation are rigid plastic foams. For sandwich panel construction, a rigid foam material with a predominantly closed cell structure is required (Davies, 2001).

The material properties of the different types of foam vary according to the raw materials used. Similarly, to polymers, polymer foams are also bi-sect into thermoplastics and thermosets, which are further divided into rigid or flexible foams. The thermoplastics can usually be broken down and recycled, while thermosets are harder to recycle because they are usually heavily crosslinked.

Issues facing the polymer foam industry are those of waste disposal, recyclability, flammability and the effect of blowing agents onto the environment. The restrictions on the use of CFC's (chloro-fluoro-carbons) has become very important in making polymer foams more environmentally friendly. Advances in biodegradable foam materials are also helping to improve the recyclability and waste disposal (Sivertsen, 2007).

The polymer foams selected to be characterised in this work are a polyethylene terephthalate (PET) foam and a polyurethane (PUR) foam. The polymer used to create the PET foam is, in part, recycled. This polymer exhibits good mechanical and thermal characteristics and high elastic modulus, high glass-transition temperature (Tg), and good crystallinity and solvent resistance. The availability of foams based on PET may could be of

great interest, mainly due to the temperature range allowed by the high melting temperature (Tm) of the bulk polymer and its crystallinity (Sorrentino et al., 2010)

The thermoplastic PET foam presents significantly higher mechanical properties than typical PUR foams of the same density. Furthermore, these foams have the advantage of being recyclable. However, its cost is higher than that of the typical PUR foams (Garrido and Keller, 2015).

The use of PUR foams is widespread, representing almost of the global foam market (Smithers, 2014). One of the main applications of rigid polyurethane foams is the thermal insulation in buildings, transport and refrigeration systems, where typically the foams are the core of the sandwich panels.

2.3.2. Balsa wood

One of the greatest attributes of wood is that it is a renewable resource. If sustainable forest management and harvesting practices are followed, wood resources will be available indefinitely, since it is a natural and sustainable material.

Balsa (Ochroma pyramidale), a tropical hardwood native to the Americas, is one of the fastest growing wood species, reaching about 20 m in height and up to 75 cm in diameter in 5–8 years (Borrega and Gibson, 2015). Because of its fast growth, the wood density is very low, making balsa wood the lightest and softest of all woods on the market (Forest Products Laboratory, 2010). Density values for balsa wood typically range between 100 and 250 kg/m^3, although they can vary as much as from 60 to 380 kg/m^3 (Borrega and Gibson, 2015).

Wood structure determines wood density: in softwoods, where latewood is abundant in proportion to earlywood, density is higher. The reverse is true when there is much more earlywood than latewood. In other words, density increases as the proportion of cells with thick cell walls increases. However, in hardwoods, such as balsa, density is dependent not only on fibre wall thickness, but also on the amount of void space occupied by vessels (long tubular structures that run axially along the trunk) and parenchyma (second type of cells that are radially arranged in groups that periodically penetrate the tracheids (rays), see Figure 2.7. In balsa wood, vessels are large (typically >250 μm in tangential diameter) and there is an abundance of axial and ray parenchyma (Borrega et al, 2015).

The low density is extremely valuable in applications that require lightweight materials with good mechanical performance. For this reason, it is one of the preferred core materials in structural sandwich panels, in applications ranging from wind turbine blades to boats and aircraft (Borrega and Gibson, 2015).

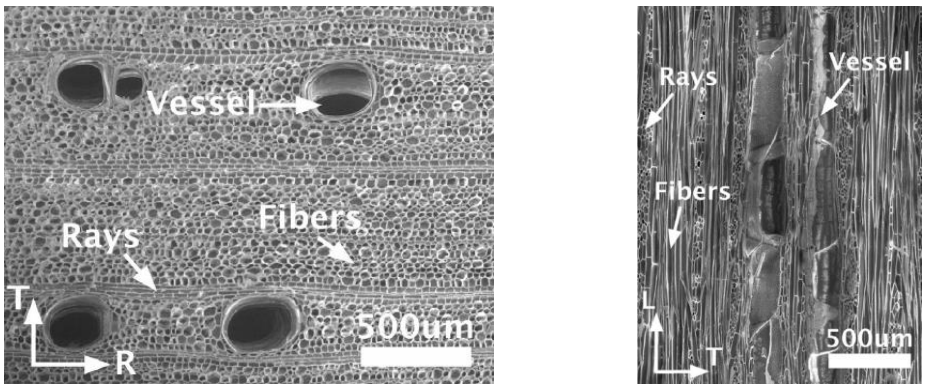

a) b)

Figure 2.7. SEM micrographs of balsa wood showing the main type of cells in: a) Cross-section; b) Longitudinal view. L, R and T refer to the longitudinal, radial and tangential axes of symmetry (Borrega et al, 2015).

As a core material, the panels are small blocks of balsa wood commonly glued together side by side to form sheets of the so-called end grain balsa, in which the grains are oriented through the thickness (Grenestedt and Bekisli, 2003). This option has a reason: first, the fibres (and the principal direction of stiffness) are perpendicular to the faces; and second, the humidity is primarily spread along the fibres and hence damage will only cause localised humidity damage. The inconvenience is that all the small balsa blocks have different densities and the design limit must hence be taken from the piece having the lowest properties. End-grain balsa is only available in a limited number of densities and thicknesses. The mechanical properties, even though restricted to the minimum density, appear quite good and higher than most cellular plastics (Zenkert, 1995).

Wood is considered to be an orthotropic material, the three axes of symmetry are the longitudinal (L, along the fibres), radial (R, along the rays), and tangential (T, across the rays).The stiffness and strength in the grain direction are considerably higher than in any other direction (Grenestedt and Bekisli, 2003).

The study of the mechanical behaviour of this type of solution has been undertaken over the years. Huiyuan et al. (2018) performed four-point bending static and fatigue experiments on composite sandwich beams with glass fibre reinforced polymer (GFRP) face sheets and Balsa wood cores. The results showed that the sandwich beams under four-point bending, both static (fatigue tests) and not static (bending tests) failed due to core shear and debonding. The study showed that to sustain at least one million cycles, the service load should be limited to 60% of the ultimate load. Li et al. (2019) also studied the flexural creep behaviour, and started out by preforming static three-point bending tests for the beams, followed by bending creep tests (based on the principle of leverage). Creep experiments were carried out for a period of 3000 h at four different load levels corresponding to 20%, 40%, 60% and 80% of the ultimate bearing capacity. The findings show that the creep behaviour exhibits linear viscoelastic properties when the load level is less than 40%, while creep failure occurs in all specimens at load levels of 60% and 80%. Specimens subjected to the 60% load level presented two failure modes, core shear failure and overall bending failure while specimens subjected to the 80% load level exhibited only bending failure.

Regarding shear, Osei-Antwi et al. (2013) studied the effects of parameters such as shear plane, density and adhesive joints contribution on the shear stiffness and strength of balsa wood panels as well as the variation of ductility with respect to the shear planes. They concluded that shear planes exerted a significant effect on shear stiffness and strength. The highest values were obtained for the shear plane parallel to the end grain, intermediate values were obtained for the plane parallel to the flat grain and the lowest values for the plane transverse to the flat grain. The thin adhesive joints in the balsa panels between the lumber blocks mostly increased the shear stiffness and strength.

Another important property for sandwich constructions, is the resistance to compression. Silva and Kyriakides, (2007) concluded that, under compression in the axial direction, the material (balsa wood) exhibits a linearly elastic regime that terminates by the initiation of failure in the form of localized kinking. Subsequently, under displacement-controlled compression, a stress plateau is traced associated with the gradual spread of cells crushing throughout the material. The material is less stiff and weaker in the tangential and radial directions. Compression in these directions crush the tracheids laterally but results in a monotonically increasing response, typical of lateral crushing of elastic honeycombs. The

elastic and inelastic properties in the three directions have been established experimentally as a function of the wood's density.

2.3.3. Mineral Wool

Mineral wool is a non-metallic, inorganic product manufactured from a carefully controlled mix of raw materials, mainly comprising either stone or silica which are heated to a high temperature until molten. The molten glass or stone is then spun and formed into a flexible, fibrous mat for further processing into finished products Mima (2020).

The thermal performance of mineral wool, which correspond to 60% of the European insulation market EURIMA (2006), is mainly due to prevention of convection by the entrapment of air in the material's open-cell, woolly matrix. Conduction is reduced because there is very little solid material to provide pathways and the trapped, static air has a low thermal conductivity. The thermal efficiency, does not rely on injected gas that can leak and result in a deterioration in thermal performance, such as in the case of polymer foams Mima (2020).

Linear temperature-dependent laws have been occasionally proposed for inorganic fibrous materials such as fiberglass or rock wool that exhibit a decreased thermal conductivity (better performance) at low temperatures. Berardi and Naldi, (2017), quantified the impact of the temperature dependency of the thermal conductivity in exterior walls and flat roofs over a certain range (from −20◦C to +60◦C) for different insulating materials. For most materials, the relationship between conductivity and temperature is nearly linear. However, some materials, such as the blown foam insulations exhibit non-linear relationships between conductivity and temperature

Possible problems with rock wool's thermal performance lie with its hydrophilic nature, which allows for water absorption and thus for an important increase of its thermal conductivity. Berardi (2019) adverted for the risks of significant differences between theoretically fixed thermal conductivity values and effective ones occurring for any porous material, including mineral fibres. Karamanos et al (2008) studied the sensitivity of rock wool when water vapour condenses in the material. As the theoretical approach predicted, the material's thermal conductivity values were significantly affected due to vapour

condensing between its fibres. Jelle (2011) suggest that the thermal conductivity of mineral wool may increase from 37mW/(mK) to 55mW/(mK) with increasing moisture content from 0 vol% to 10 vol%.

Although the mechanical performance is not the main feature of mineral wool, it is required that it maintains integrity during its service life. Karamanos et al (2008) noticed that long-term presence of water in the material, or the material's prolonged exposure to high temperatures, may affect the resins used to hold the fibres together. The degradation of fibres begins when the increase of the thermal conductivity factor becomes non-linear with respect to temperature or relative humidity. In that case, rock wool's compressive and tensile strength values may be significantly weakened, leading to structural failure.

2.4. Climatic chamber requirements

The increase in the demand for high quality products has led to a surge in tests that use climatic chambers, and the requirements set for these tests have become stricter. Application like the ones in the automotive, electronics and the aeronautic sectors require very strict durability tests see Figure 2.8. For instance, aeronautic applications are subject to extreme temperatures during flight or when parked at airfields worldwide. Single parts, subcomponents or complete systems should be tested and validated for use in these extreme conditions.

Figure 2.8. High performance and large-scale examples of climatic chambers for testing. Sirris (2020).

Depending of the product being tested, the dimensions of the chambers can be very large, creating new challenges for the structure, the insulation, safety, air flux efficiency, etc. This kind of equipment should be studied in order to optimise its performance and for energy saving. Apart from technological component of the climatic chamber such as fans, thermal resistances, compressors, etc., its efficiency should also be studied based on its shell. Using fluid dynamic analysis Silva et al. (2020), calculated the thermal heat losses for the various components of a climatic chamber (300 dm^3). This analysis of the equipment was performed for an inner temperature of 120°C, and an external temperature of approximately 20°C. It was verified that the greater percentage of heat loss was from the walls, through the insulation, representing 88.5% of the total value. This is due to their large surface area when compared with other elements such as thermal bridges. This study demonstrates de significance of the shell in the thermal performance and energy efficiency of a climatic chamber.

2.5. Temperature influence on the mechanical behaviour of core materials

In many applications, sandwich panels are likely to be subjected to relatively high in-service temperature gradients (e.g., facade panels, roof structures, bridge decks, climatic chambers). From a design standpoint it is particularly important to obtain an adequate understanding on how the mechanical properties of their materials are affected by these in-service temperatures.

Zhang et al. (2015) established an experimental apparatus which enabled the investigation of sandwich beam specimens of PVC foam and aluminium sheets. The specimens were subjected to a simultaneous simply supported four-point bending load and

a linear temperature gradient along its thickness. To assess the occurrence and rapid evolution of face sheet wrinkling, the strains were determined from measured displacements obtained from digital image correlation, which provided a good approach to assess the occurrence of face sheet wrinkling. It was experimentally observed that the specimens failed by face sheet yielding at room temperature and by wrinkling (instability) when the top face sheet was heated to 70 ºC or higher.

Garrido et al. (2015) presented an experimental and analytical study about the effects of high temperature on the shear response of polyethylene terephthalate (PET) and polyurethane (PUR) foams used in composite sandwich panels. The results obtained showed that the shear responses of PET and PUR foams become more markedly nonlinear with the increase of temperature. Pulngern et al. (2016) analysed the effect of temperature on mechanical properties and tensile creep responses of Wood/PVC composite materials.

The polymeric materials are more sensitive to temperature. However, this concern applies to other materials as well. Vahedia et al. (2016) characterised (thermally and mechanically) balsa-wood-veneer structural sandwich core material at elevated temperatures and the results showed that independently of the loading type, the specimens gradually lost strength and stiffness up to the wood-burning temperature of 250ºC, due to the softening of the hemicellulose and lignin. Goodrich et al. (2010) also investigated the temperature effect on balsa. The study focused on the thermal softening response of balsa with increasing temperature, and the thermal recovery behaviour when softened balsa is cooled following heating. Exposure to elevated temperatures was limited to a short time (15 min), representative of a fire or post-fire scenario. The compression strength of balsa decreased progressively with increasing temperature from 20° to 250°C. The degradation rates in the strength properties over this temperature range were similar in the axial and radial directions of the balsa grains. The reduction in compression properties is attributed mostly to thermal viscous softening of the hemicellulose and lignin in the cell walls. The microstructure of balsa was analysed using scanning electron microscopy. The results showed minor physical changes to the wood grain structure from 190° to 250°C, with holes beginning to form in the cell wall at 250°C. Post-heating tests revealed that thermal softening up to 250°C is fully reversible when balsa is cooled to room temperature. When balsa is heated to 250°C or higher, the post-heating strength properties are reduced significantly by decomposition processes of all wood constituents, which irreversibly degrade the wood's microstructure.

2.6. Temperature influence on the thermal behaviour

Low-density materials used for sandwich cores typically have very low thermal conductivity, conferring thermal insulation properties to the panels.

Tabulated values of thermal properties of insulation materials are available in the literature. The accuracy of the thermal properties provided by the manufacturers is questionable since sometimes it is incomplete. Thermal conductivity is the most common value available in technical sheets, but mostly is given without providing the material's density and the temperature at which it was tested.

The thermal conductivity of an insulation material not only depends on its density, temperature and moisture content, but it also depends on the material's atomic and molecular structure, porosity, anisotropy, structural faults and defects (Al-Ajlan, 2006). The effect of temperature on thermal conductivity is often dismissed and the values used as reference do not take this effect into consideration. The service temperatures of the main applications of sandwich panels can be substantial and the thermal behaviour of these construction elements can be well below the expectations. Berardi (2019) studied the impact of ageing and environmental conditions on the effective thermal conductivity of several foam materials. Results showed that the ageing of the foams and the operating temperatures have high impact. Additionally, it was concluded that high moisture levels contribute to lower performance in all foam materials, with open cell foams experiencing the greatest thermal resistance reduction. Measurements in pristine conditions confirmed the superior performance of these materials when tests are performed according to traditional tests for the measurement of the thermal conductivity.

Thermal conductivity and transmittance are used to define the insulation properties in steady state. For the unsteady state, the parameter most used to compare the ability of materials to conduct and store thermal energy is thermal diffusivity (m^2/s). It is given by the ratio of thermal conductivity and the product of density and specific heat. This parameter, specific heat, is not usually presented by manufacturers. However, it is very important for thermal simulation and energy efficiency evaluation.

A material characterised with a high specific heat value can provide low diffusivity values even with low density. Insulation materials characterised by thermal

conductivity under 0.05 W/mK and specific heat over 1.4 kJ/kgK can be considered to have great performance, even in unsteady state conditions. (Asdrubali et al., 2015)

The temperature effect on thermal conductivity has been studied for most conventional insulation materials. For instance, (Zang et al., 2017) presented an experimental study on the thermal insulation performance and radiative property of five different PUR foams, produced using different blowing agents. The thermal conductivities of the five studied foams increased non-monotonically with temperature because the increase of temperature will promote gases within the closed cells diffusing out and as result the thermal conductivity increases. When stored in moist air, PU foams will absorb water vapor from the air and result in weakened thermal insulation capacity. Thermal conductivity and water uptake increase with humidity at different temperature. The water uptakes of the five foams were less than 2% at different temperature and humidity but the increase of thermal conductivity was as high as 10–18%. The thermal conductivities of PU foams increased by 8–12% at 20ºC after being submitted to -40ºC and 70ºC alternately for a week. Long term storage of PU foam (at 40ºC for a week) resulted only in 1.6–3.8% increase of the thermal conductivity.

The interest of studying temperature influence on thermal behaviour is also shown for natural materials. (Huang et al., 2018) studied the heat and moisture transfer behaviours in the Phyllostachys edulis (Moso bamboo) panels at various temperature and relative humidity (RH) conditions: 10ºC to 35ºC and 10% to 90%. The results indicated that, although the panel made from layers of the internal part of bamboo culm wall can provide good insulation performance, its ability to resist high RH variation is inferior to the layer from the external part of bamboo culm wall. The results of this study demonstrated that the external part of the bamboo culm wall can be used to minimise the RH variation of the panel while the internal part is suitable for increasing the thermal insulation performance of the panel.

3. THERMAL CHARACTERISATION

3.1. Experimental methodology

In order to allow the performance of tests under conditions that are similar to those of real applications, it was necessary to develop an experimental setup where one of the surfaces of the specimens is submitted to high temperature, while the other faces the indoor room laboratory temperature. This creates a thermal gradient, that generates a heat transfer between both environments.

The purpose is to determine the effect of temperature on the thermal conductivity and specific heat. The test procedure includes steady state (for predefined temperature levels) and unsteady state periods, resulting from the temperature level transition. The oven's temperature only increased to the next temperature level after 6 hours in order to allow for a steady state regime to be reached. The temperature steps were: 40ºC, 80ºC, 120ºC, 160ºC, and 200ºC.

This was achieved by adapting an oven (see Figure 3.1). The original doors of the oven were replaced by another set designed for this test. The modification consisted in creating two openings, one for each door/specimen, with large insulated walls accommodate of test specimens with different thickness and to also allow for specimen deformation. The specimens are simply supported on two rollers with an adjustable position. A detailed drawing of the oven adaptation is presented in annex A.

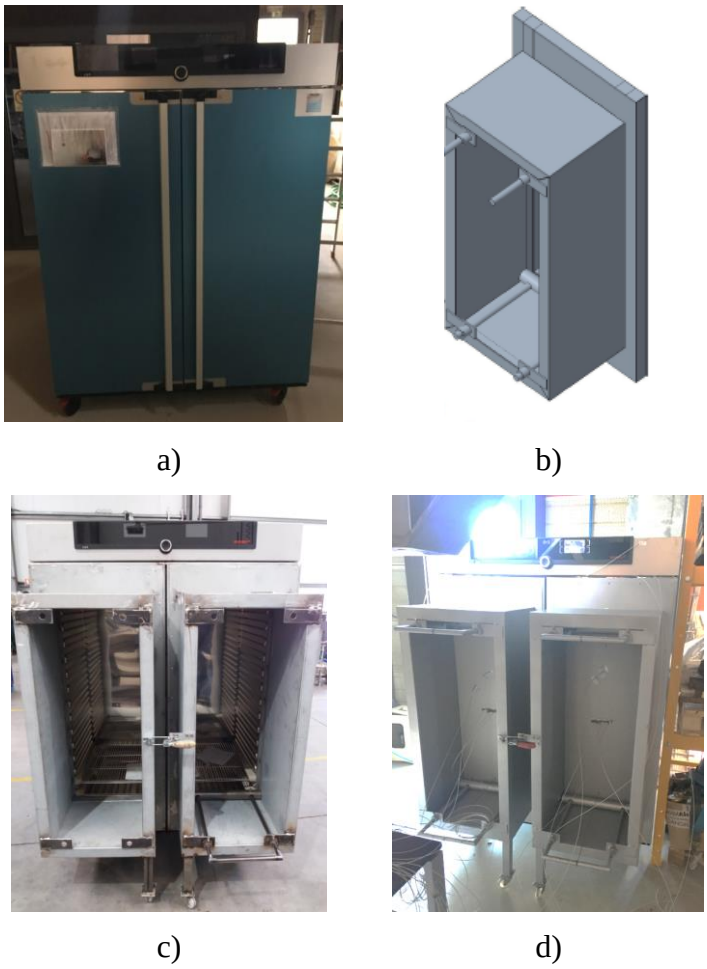

Figure 3.1. Oven adaptation: a) Photographic register of the original oven; b) Drawing of the door adaptation; c) Photographic register of the adapted equipment; d) Photographic register of a test.

The set up allows the simultaneous to testing of two specimens of the same core material, one on each door (left door specimen and right door specimen). Sandwiches with a single core layer (stainless-steel sheet – core material – stainless-steel sheet) were tested. Different core materials were selected, two polymer foams (PET and PUR), balsa wood, and mineral wool, (see Figure 3.2). The stainless-steel sheets were kept with the same thickness (0.7 mm), while the thickness of the core layer changed accordingly to the type of material, given that it was not possible to standardize the thickness of the test specimens.

Nominal thickness: 60 mm	Nominal thickness: 150 mm	Nominal thickness: 60 mm	Nominal thickness: 48 mm
a)	b)	c)	d)

Figure 3.2. Photographic record of the test specimens: a) MW core: b) PUR core; c) PET core; d) Balsa wood core.

To evaluate the variation of the thermal conductivity and specific heat with temperature, a set of thermocouples were used to record the temperature, inside and outside the oven (Ta and Tb, respectively) and across the tested specimens (T1 to T5), (see Figure 3.3). The thermocouples were placed according to the following: T1 on the internal panel surface, T2 a quarter way into the core material, T3 halfway into the core, T4 at another quarter way into the core, and T5 on the external panel surface. Efforts were made to ensure that the thermocouples are equidistant and that there are only minor deviations. The distances between thermocouples, L1, L2, L3 and L4 were measured before making the holes for the thermocouples and at the end of the test.

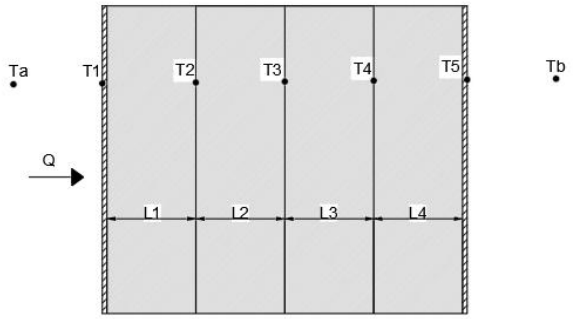

Figure 3.3. Schematic representation of test specimen (side view), where Ta and Tb represent the thermocouples exterior position (inside and outside the oven, respectively), T1 to T5, the thermocouples in the panel, Li the thickness of the interior layers, and Q the heat flux with the direction indicated by an arrow.

For placing the thermocouples, as a first approach, small holes (with a diameter of 3 mm) were drilled on the external surface, perpendicularly to the test panel, at different depths (as already mentioned), (see Figure 3.4a)). However, this setup did not work, since the vertical hole was found to markedly perturb the heat transfer across the test specimen. As a second approach, the holes were drilled on the lateral side of the panel along the parallel direction of the test specimen (see Figure 3.4b). This option brought an additional difficulty in making the holes, since the depth needed was much bigger (approximately half of the panel's width). The problem was solved by using a long drill. The thermocouples are not aligned to avoid the effect from the neighbouring holes on the results, as shown in Figure 3.1.

Figure 3.4c) shows the interior view of the door with a specimen assembled. The panel is smaller (990 mm x 390 mm) than the door opening (1000 mm x 400 mm) to allow for the thermal expansion of the test specimens. The gaps between the test specimen and the door opening were filled with a ceramic fibre to prevent heat loss during the test.

a) b) c)

Figure 3.4. Photographic record of the setup (thermocouples marked in red and heat flux sensors in green): a) First approach (thermocouple holes on the front): b) Second approach (thermocouple holes on the lateral side); c) Interior view of the door with a specimen assembled.

Apart from temperature acquisition, heat flux was also recorded. For this, two heat flux meters were placed on each exterior panel's surface, as can be seen in Figure 3.4b).

The data acquisition (temperature and heat flux) was carried out continuously during the test to allow for the determination of thermal conductivity in each layer for each temperature step. Specific heat was also calculated considering the estimated thermal conductivities and the transient periods data. The detail and the assessment basis are explained next.

As a complement, the thermal conductivity of the core materials at 10 ^{o}C was also determined experimentally, in accordance with the standard EN 12664, in de case of balsa, and EN 12667, for the remaining materials. Details regarding the samples, test procedures and equipment are provided in annex B.

3.2. Results and discussion

Figure 3.5 shows the temperature and heat flux recorded during the test for the different specimens.

Left door **Right door**

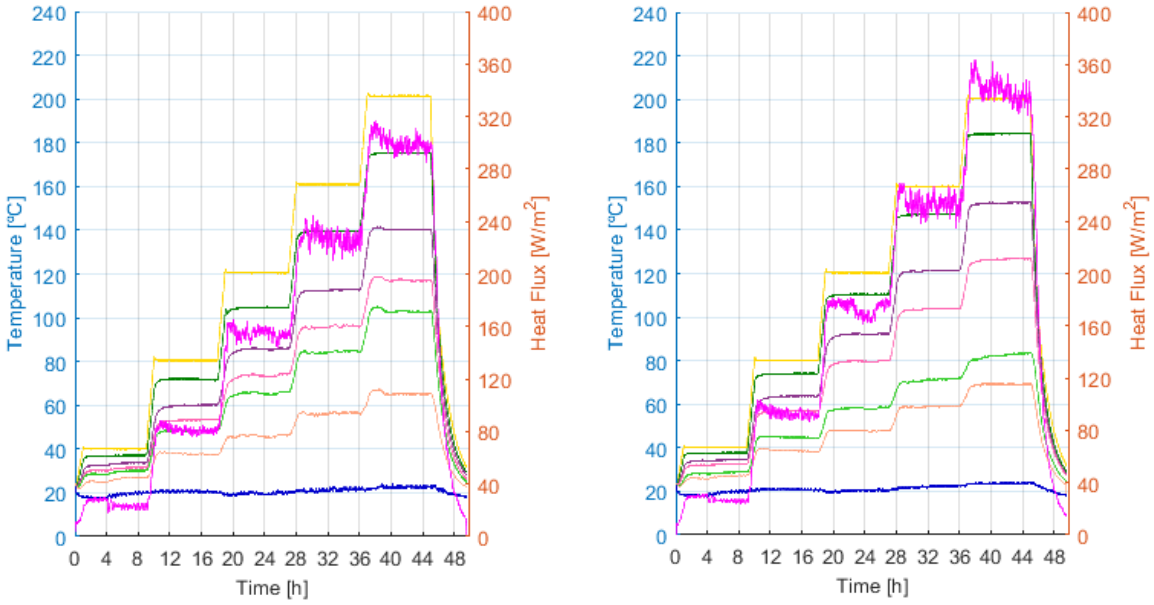

a)

Left door **Right door**

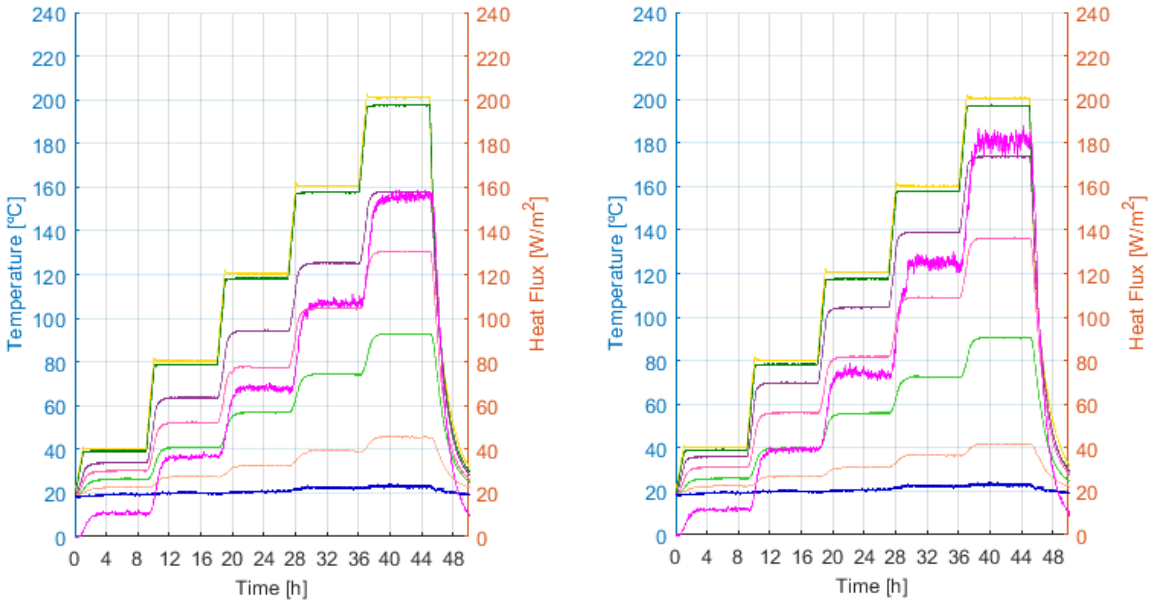

b)

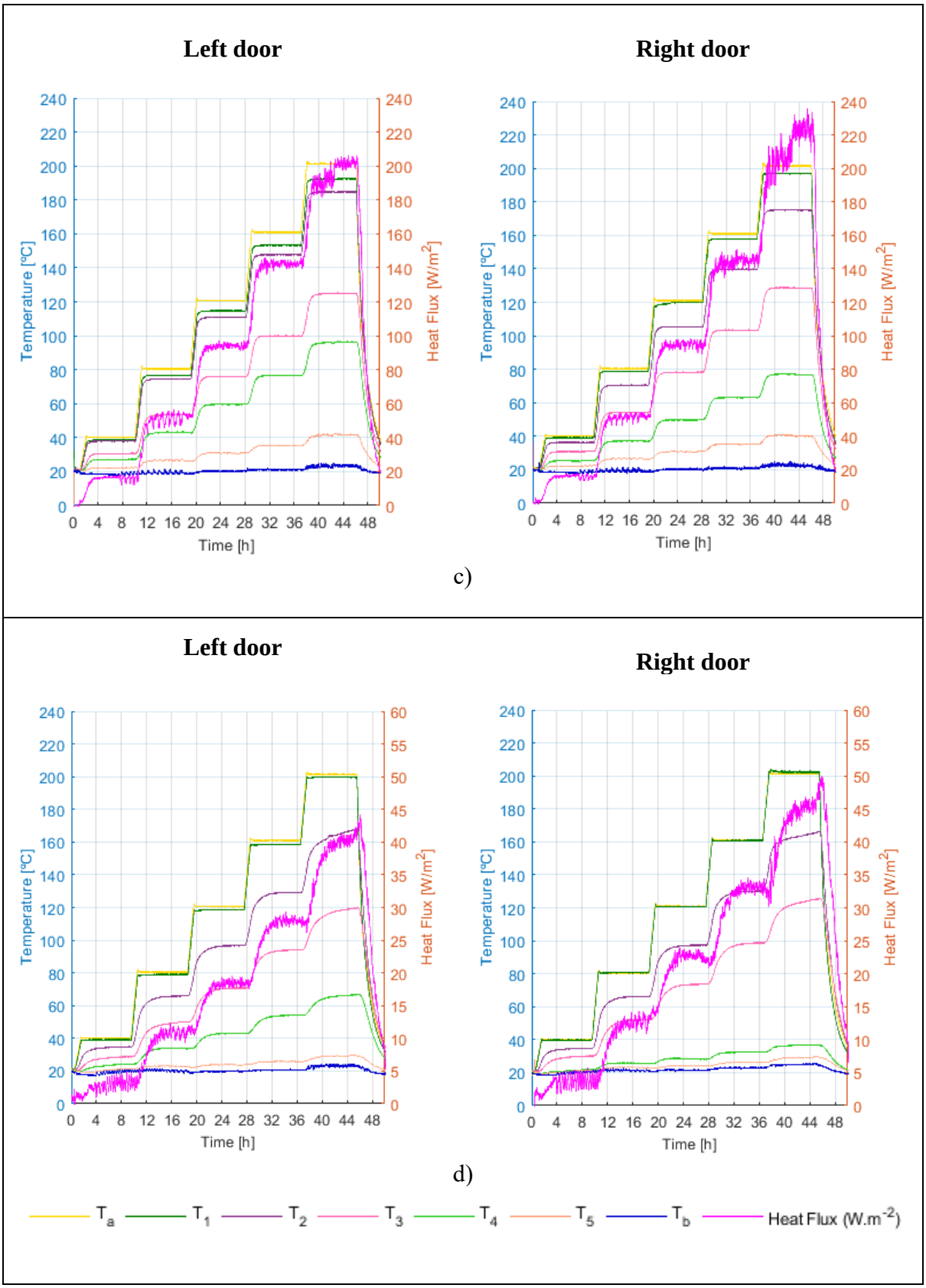

Figure 3.5. Temperature and heat flux recorded during the test (left door in the images on the left and right door in the images on the right): a) Balsa panels; b) PET panels; c) MW panels; d) PUR panels.

In order to determine thermal conductivity, for each temperature step it was necessary to guarantee the existence of steady state conditions (constant temperatures and heat fluxes). Figure 3.6 presents, as an example, the temperature and heat flux recorded in the steady state, for each temperature step, for a left door with PET panel.

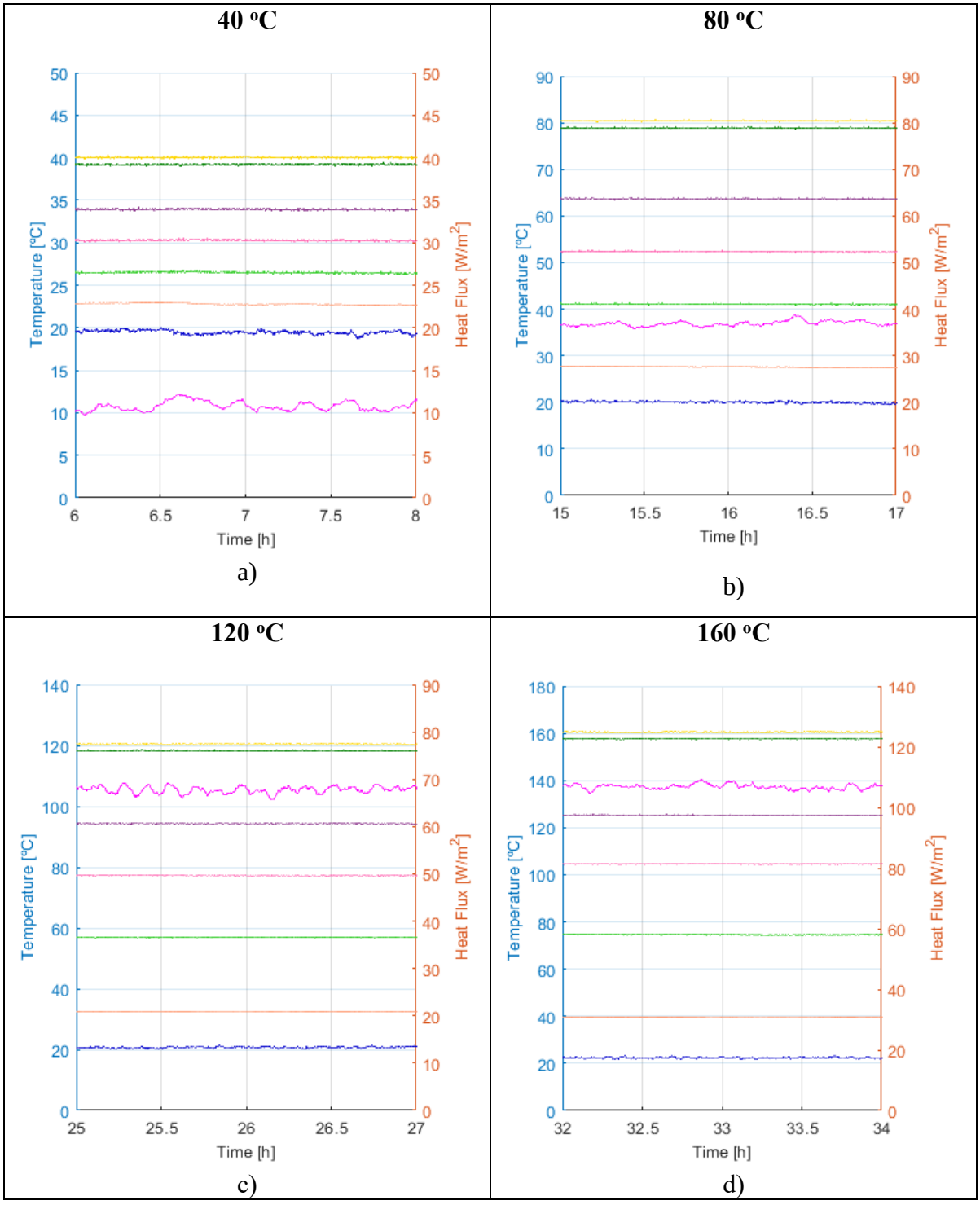

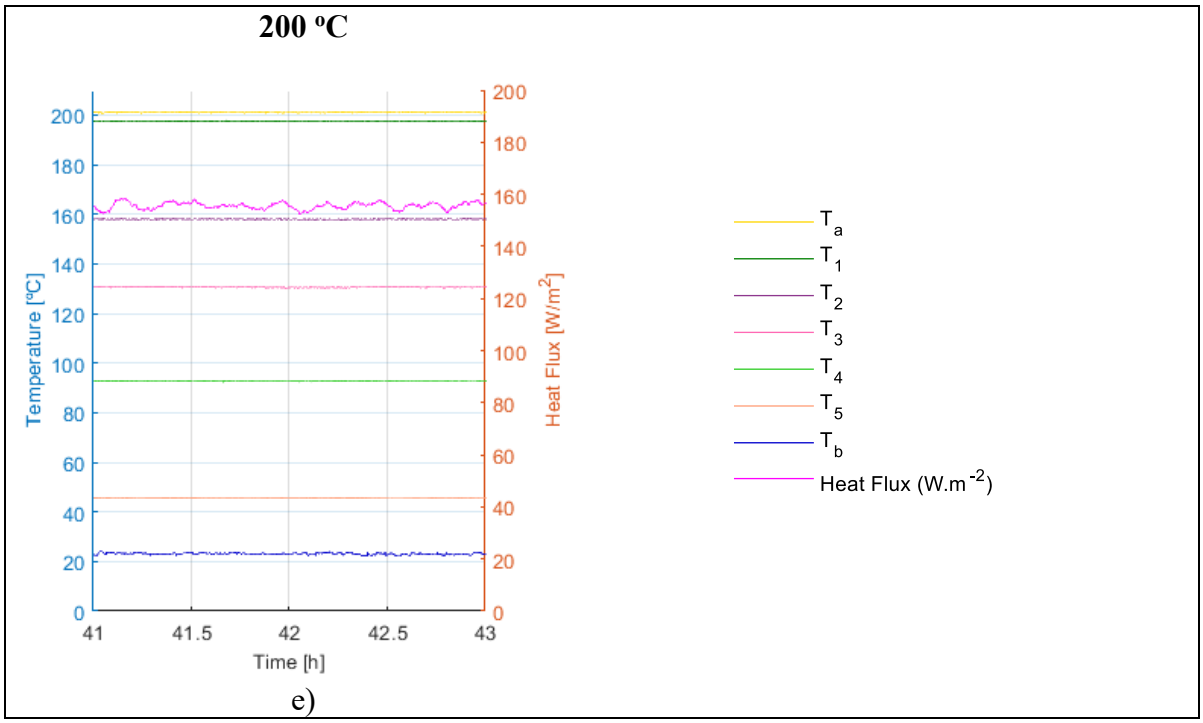

Figure 3.6. Temperature and heat flux record in the steady state for the PET panel, left door: a) Step 40 ºC; b) Step 80 ºC; c) Step 120 ºC; d) Step 160 ºC; e) Step 200 ºC.

Under conduction conditions, the heat flux ($W \cdot m^{-2}$) is adequately described by Fourier's law:

$$\phi_q = -\lambda \frac{\Delta T}{\Delta x} \qquad (3.1)$$

Fourier's law of thermal conduction states that the time rate of heat transfer through a material is proportional to the negative gradient in the temperature and to the area. The proportionality constant obtained in the relation is known as the thermal conductivity, λ, of the material. Nevertheless, there are some assumptions of Fourier's law of heat conduction, namely, that conduction takes place under steady state conditions; the heat flow is unidirectional; there is no internal heat generation, and the material is homogeneous and isotropic.

Thermal conductivity can be calculated with test data, considering that ΔT corresponds to the temperature difference between consecutive thermocouples located at a distance of Δx. The negative sign shows that heat flux moves from higher temperature regions to lower temperature regions.

The thermal conductivity was determined for the two interior layers (L2 and L3) shown in Figure 3.7, since the contiguous material is the same (core material). The exterior layers L1 and L4 comprise of a double layered system, since these incorporate the steel sheets. The thermal conductivity, λ2, was determined considering ΔT=T3-T2 and Δx=L2, and following the same rational, λ3 was determined considering ΔT=T4-T3 and Δx=L3.

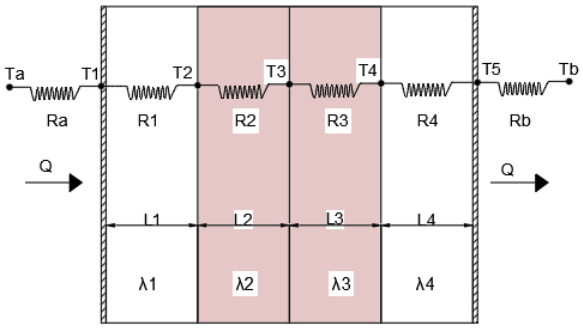

Figure 3.7. Identification of the variables.

Figure 3.8 presents thermal conductivity as a function of the oven interior temperature, for each core material. The left door specimen results are presented in yellow (asterisk marker) and the right door in blue (circle markers). The left column has the graph of the L3 layer (which is more distant from the oven's interior), and the right column has the L2 layer (which is closer to the oven's interior). The distance from the oven's interior to the middle of the layer in analysis, d is also indicated, d for L2 corresponds to L1 + L2/2, and for L3 is L1+L2+L3/2.

The thermal conductivity presented for each layer is an approximate value, since it varies along the layers' thickness. This approximation is more real the smaller the layer thickness considered in the calculation is. The panels do not have the same thickness and were divided in layers with an approximate thickness. For that reason, the graphs in Figure 3.8 for each material cannot be compared directly.

The thermal conductivity results for layer L2 were, for all cases, greater than those obtained for layer L3 (for the same test), since the mean temperatures in L2 were always higher than in L3 (farther away from the oven's interior). An analysis between tests/replicates can be made by comparing, for each material, the results for left/right doors (yellow and blue). However, and despite the attempt, the distance d has some variation

between the left and right specimens, due to the variation in the thickness of the layers. That difference, in spite of being small, contributes to differences in the conductibility values. The material which presents greater differences between specimen is the balsa wood panels. This is due to balsa being a natural material which can present some variance in density. Also, the balsa wood panels are made of balsa cubes unified by a mesh in one side, to accommodate the dimensional variations, a typical feature in wood. This means that it is not a homogeneous material like a massive wood beam and it has some air gaps. The thermal conductivity of wood is known to be affected by a number of basic factors: density, moisture content, extractive content, grain direction, structural irregularities such as checks and knots, fibril angle, and also temperature (Forest Products Laboratory, 2010).

For the other materials under study, the differences, while not as substantial, can be related with the difficulty of positioning the thermocouples in the right place and in contact with the material. Although the diameter of the thermocouple's holes was the smallest possible, it was difficult to ensure contact. To minimize this issue, each thermocouples' tip was embedded with thermal mass.

The results show that thermal conductivity increased with temperature. To better understand how thermal conductivity increases with temperature in each layer, Figure 3.9 presents the thermal conductivity as a function of the mean temperature ranges (T3-T2 and T3-T4) for the layers L3 and L2 (left graph and right graph, respectively). The left door specimen results are presented in pink (with asterisk markers), and the right door in a salmon colour (using circular markers).

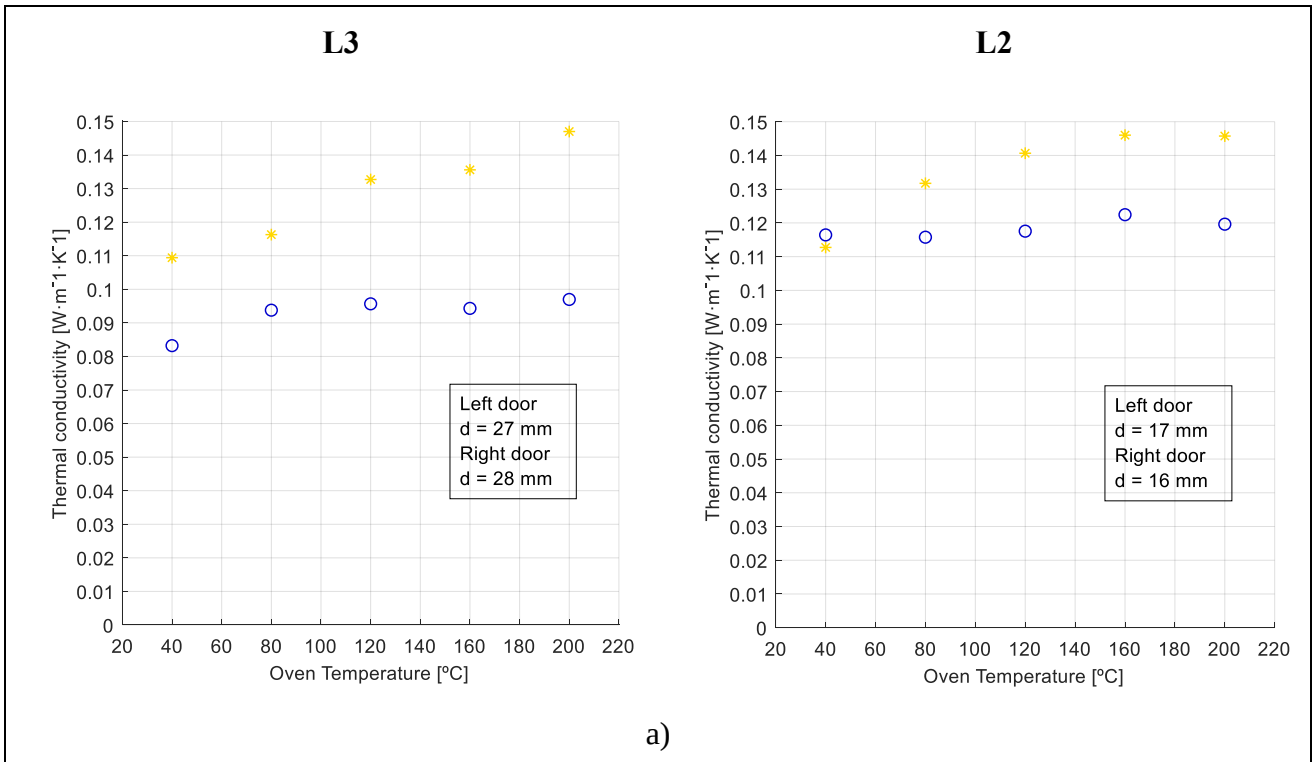
L3
L2
Thermal conductivity [W·m¯1·K¯1]
Oven Temperature [ºC]
Left door
d = 27 mm
Right door
d = 28 mm
Left door
d = 17 mm
Right door
d = 16 mm

a)

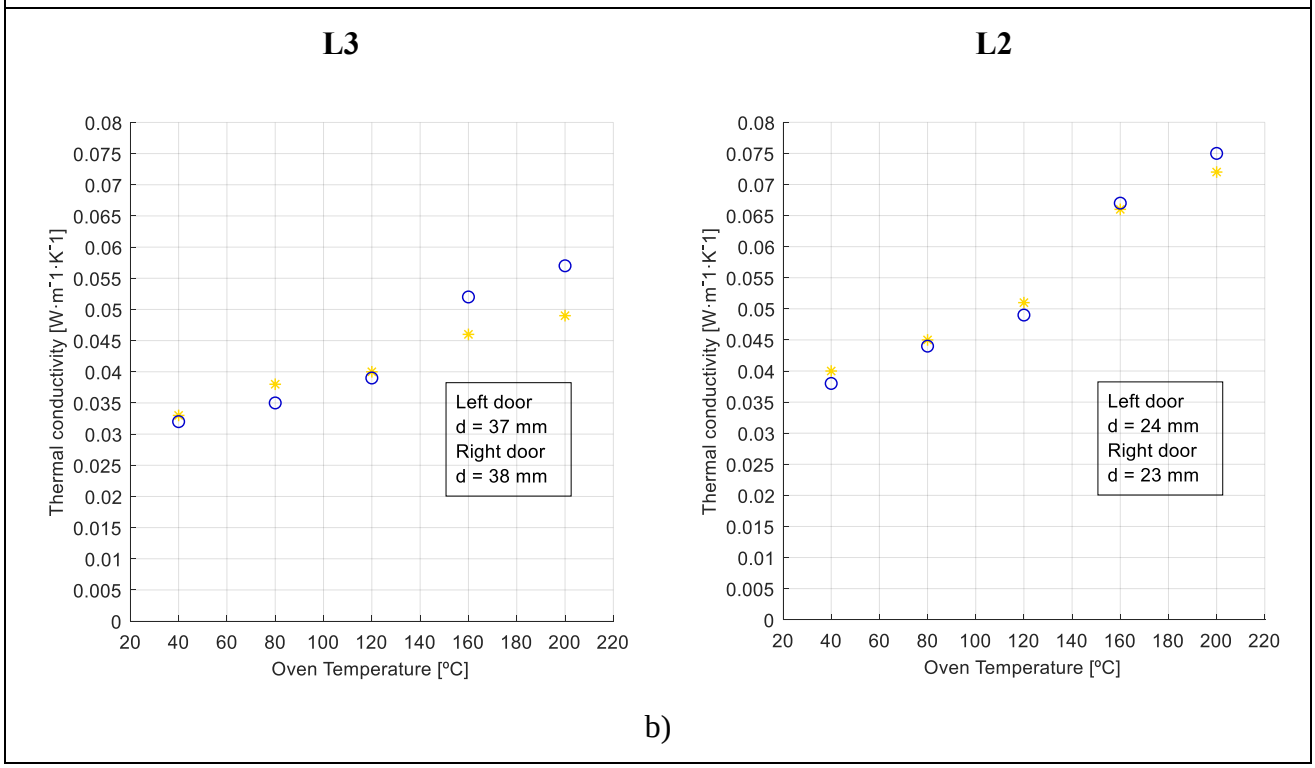
L3
L2
Thermal conductivity [W·m¯1·K¯1]
Oven Temperature [ºC]
Left door
d = 37 mm
Right door
d = 38 mm
Left door
d = 24 mm
Right door
d = 23 mm

b)

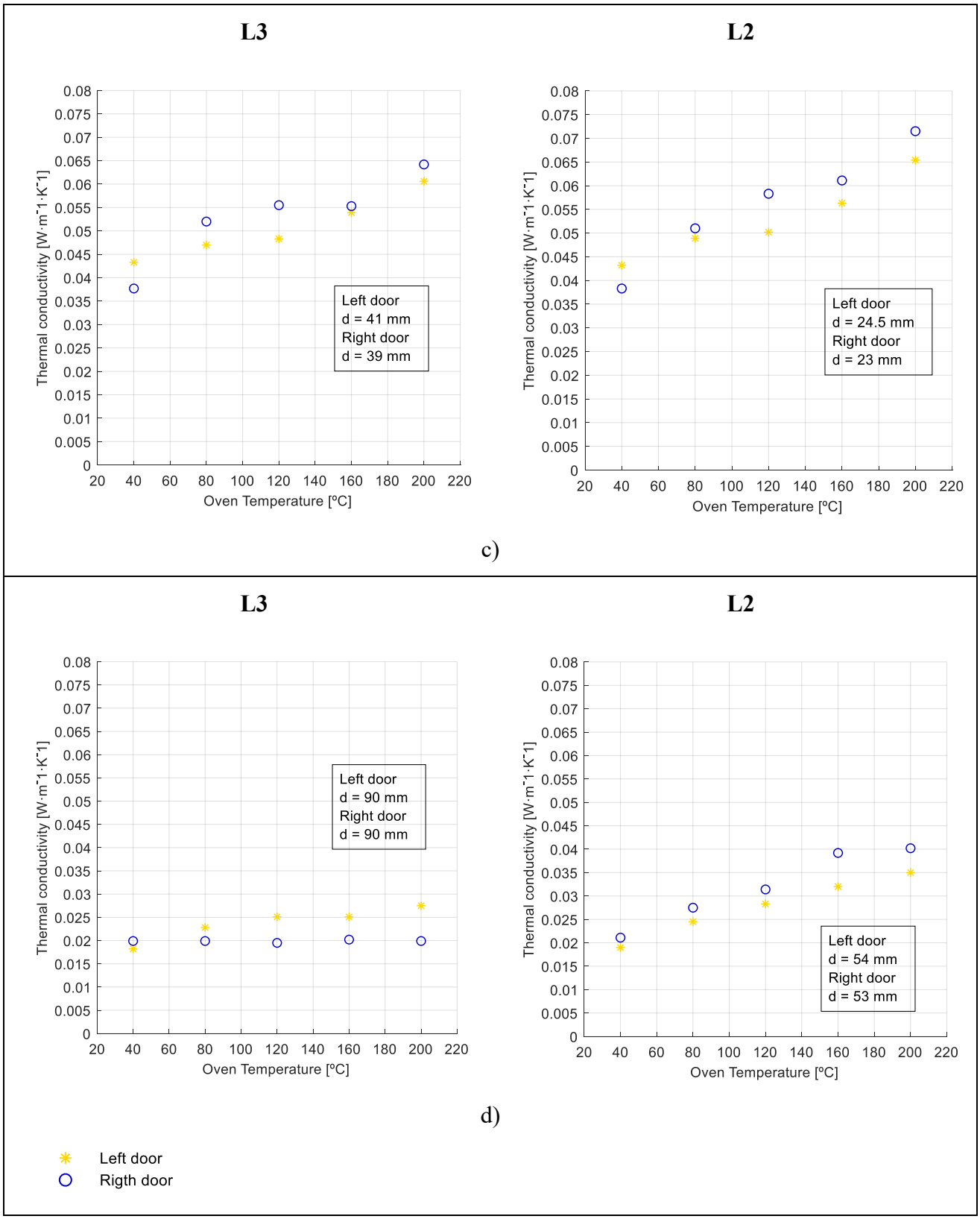

Figure 3.8. Thermal conductivity/oven temperature: a) Balsa panels; b) PET panels; c) MW panels; d) PUR panels.

Regarding the balsa results from the graphs in Figure 3.9a, it can be seen that the effect in thermal conductivity is smaller for higher temperatures, showing a non-linear behaviour. It can be noticed that for the PET specimens (Figure 3.9b), there is a leap in thermal conductivity when the oven is at higher temperatures - more significant for the layer L2, around 90ºC to 120ºC. The same leap happens for the other polymeric foam (PUR), for the same temperatures (Figure 3.9d). This can be related in both cases with some microstructural change of the material at that temperature, linked to the glass-transition temperature of the polymer.

The PUR results stabilize for the two higher temperature levels (layer L2). However, this cannot be interpreted as a non-linear behaviour since after the test it was possible to observe the deterioration of the material, which certainly may have interfered in the data acquisition/position of the thermocouples and in the results (see Figure 3.10). The moment or the temperature at which the damage started cannot be pointed out, but it certainly can be confirmed that this polymer foam cannot be used between 140ºC and 150ºC.

The thermal conductivity of the mineral wool and the PET foam presented very similar behaviour and performance. Both panels (MW and PET) have the same nominal thickness and similar initial thermal conductivity values, as well as the final ones, are close. Also, the graphs exhibit a linear behaviour more or less with the same rate.

L3

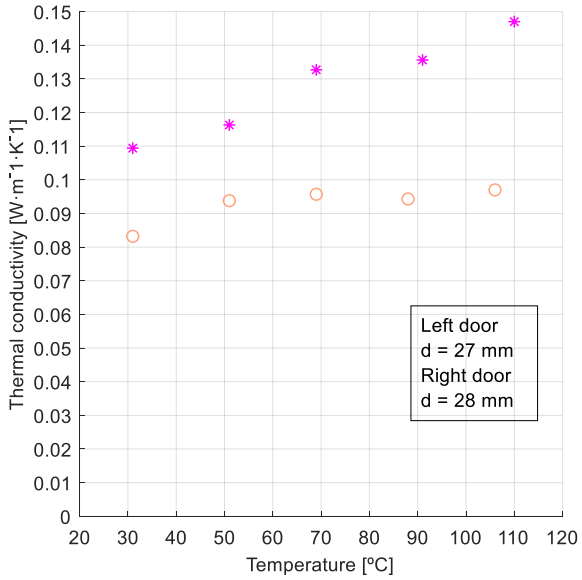
Thermal conductivity [W·m⁻¹·K⁻¹]
Temperature [ºC]
Left door
d = 27 mm
Right door
d = 28 mm

L2

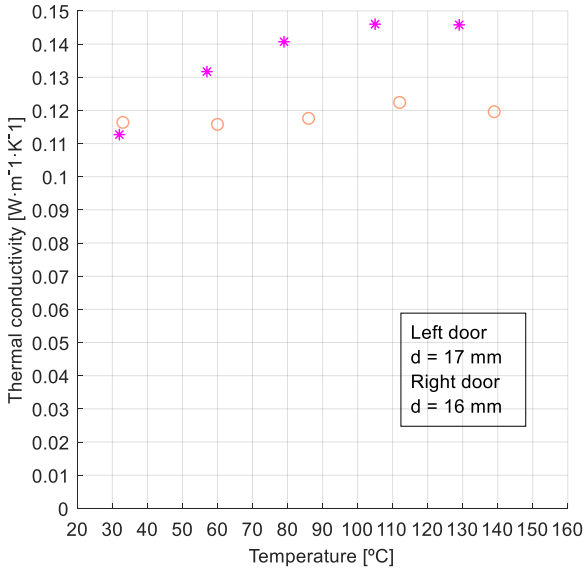
Thermal conductivity [W·m⁻¹·K⁻¹]
Temperature [ºC]
Left door
d = 17 mm
Right door
d = 16 mm

a)

L3

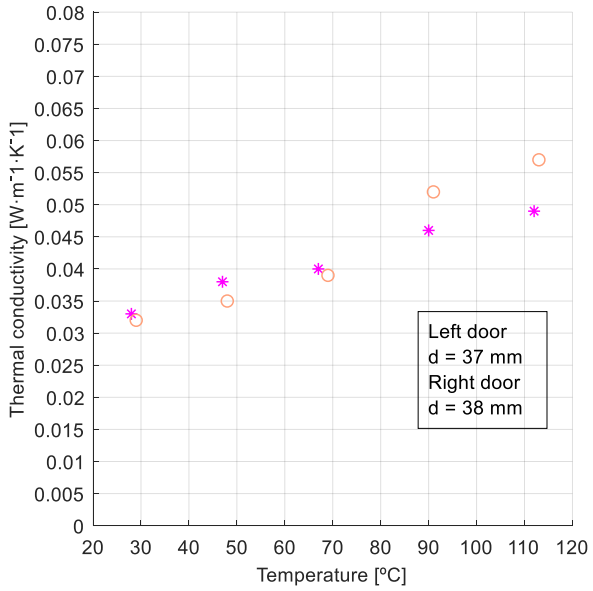
Thermal conductivity [W·m⁻¹·K⁻¹]
Temperature [ºC]
Left door
d = 37 mm
Right door
d = 38 mm

L2

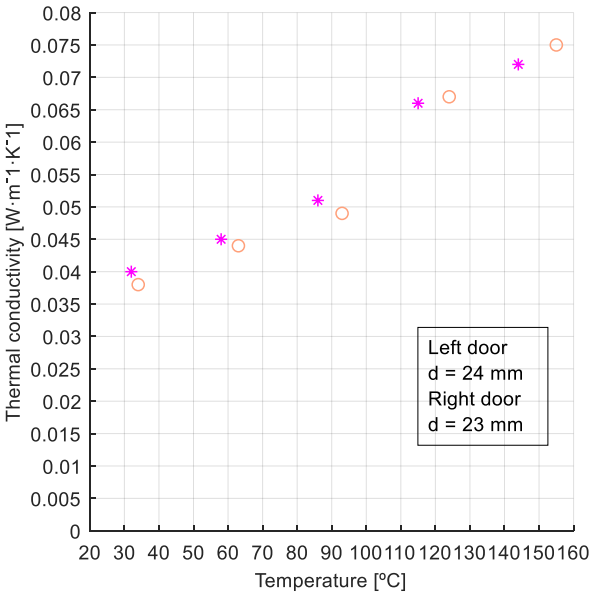
Thermal conductivity [W·m⁻¹·K⁻¹]
Temperature [ºC]
Left door
d = 24 mm
Right door
d = 23 mm

b)

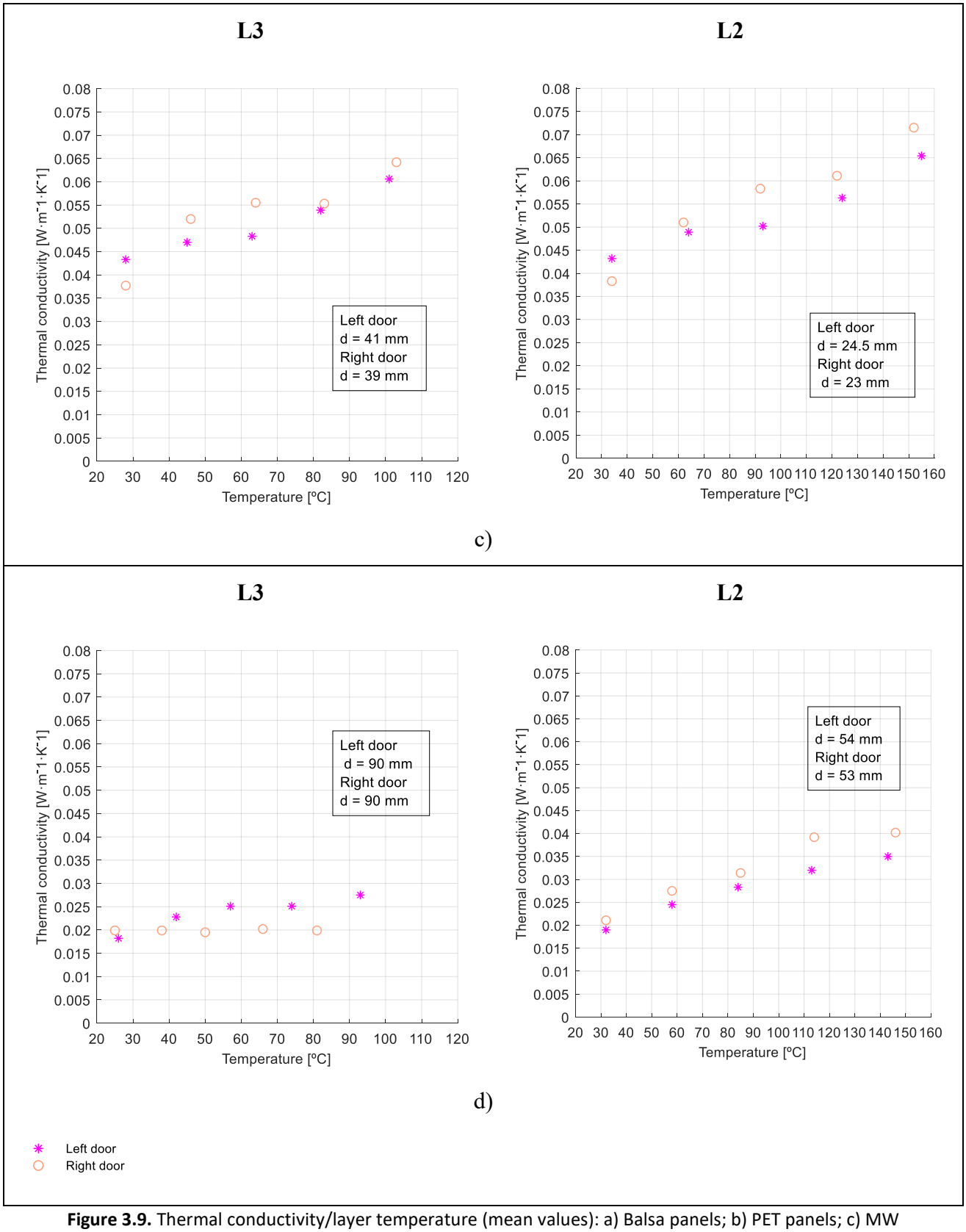

Figure 3.9. Thermal conductivity/layer temperature (mean values): a) Balsa panels; b) PET panels; c) MW panels; d) PUR panels.

a) b) c) d)

Figure 3.10. Photographic record of a section of the specimens after test: a) Balsa panels; b) PET panels; c) MW panels; d) PUR panels.

Thermal conductivity at 10ºC was also experimentally determined in accordance with the standard EN 12664, in the case of balsa, and standard EN 12667, for the remaining materials. The results are presented in Table 3.1. These results are in accordance with the thermal conductivity determined for the first temperature level, which validates the developed experimental setup. The results also show that the thermal conductivity does not vary with temperature from 10 ºC to 30 ºC.

Table 3.1: Results of thermal conductivity of the core materials at 10 ºC.

	PET	**PUR**	**Balsa wood**	**MW**
Apparent density (kg/m^3):	98.30 ± 0.46	41.2 ± 1.0	174.6 ± 30.56	120.2 ± 4.1
Thermal conductivity (W/(m.ºC)):	0.0396 ± 0.0014	0.019 ± 0.001	0.1158 ± 0.0202	0.0400 ± 0.0022

An indirect method was also used to evaluate the specific heat capacity. This method combines the experimental data with results from a one-dimensional analytical transient heat transfer model, following the methodology proposed by Simões et al (2012). The specific heat capacity was determined by aligning the experimental values registered by thermocouples with the analytical results, using an iterative approach.

The program inputs are the temperatures registered over time on the exterior faces, T1 and T5, and the middle temperature, T3 (see the thermocouples positioning scheme

in Figure 3.7). Two layers between the three thermocouples were defined: a first layer (closer to the oven's interior), which corresponds to (L1+L2); and a second layer (more distant from the oven's interior), which corresponds to (L3+L4). Besides the mentioned temperatures (over time), the other data required for the simulation were the positioning of the thermocouples, the thickness of the layers and the characterisation of the materials. This consists in defining the following thermal properties: specific heat (an initial value to start out the iterative process; density; and thermal conductivity (using the mean values obtained previously). Taking this data into account, the program does a reversive analysis and converges towards a specific heat value that corresponds to the best fit.

Figure 3.11 exemplifies the temperature input for the numerical simulation. Each simulation was carried out for each temperature step, considering the stable part of the previous step (for example, 40ºC in the case of the Figure 3.11), the transient phase, and the stable phase of the step (in this case 80ºC). Besides the inputs, Figure 3.11, presents the final output of the program (blue crosses) which correspond to a T3 temperature convergence. As it can be seen, the blue crosses coincide with the input data. The best fit specific heat value will correspond to the smallest mean squared error between the two temperature results (the T3 input and the program result).

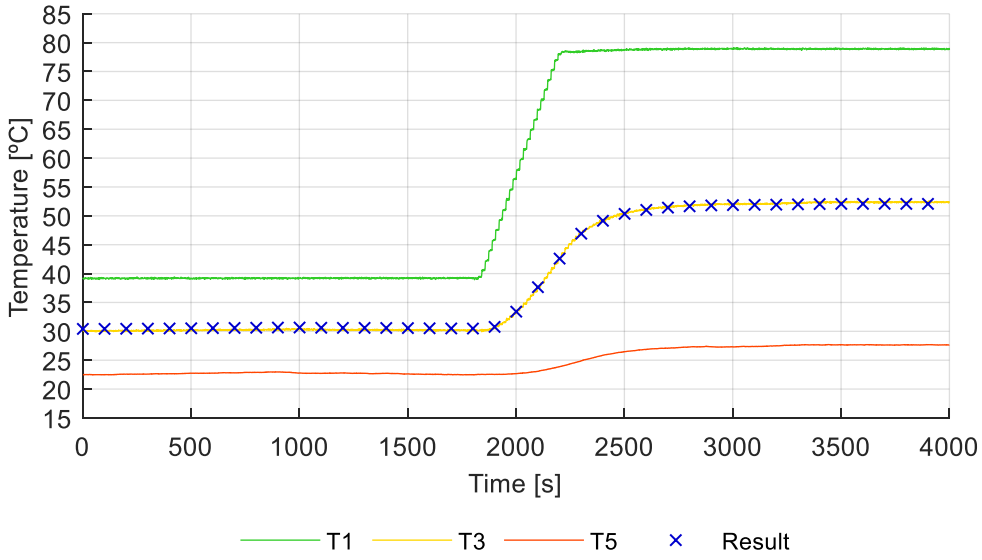

Figure 3.11. Example of the temperature input and output of the numerical simulation for the PET panel, left door, transient state between 40ºC and 80ºC temperature steps.

This process was repeated for each temperature (5 steps), for all the test specimens. Table 3.2 presents the mean value of specific heat for each material and each temperature step. The results are also presented in a graphic form in Figure 3.12.

Table 3.2: Results of specific heat capacity $[\boldsymbol{J/(kg.K)}]$ of the indirect methodology.

Ovens' temperature	Mean Temperature T3	PUR	MW	PET	Balsa wood
40	31 ± 1.4	1470	843	1822	1212
80	53 ± 2.9	1755	1023	1864	1306
120	77 ± 3.3	1799	1193	1970	1399
160	103 ± 2.7	1794	1291	2325	1513
200	128 ± 2.1	1820	1310	2534	1609

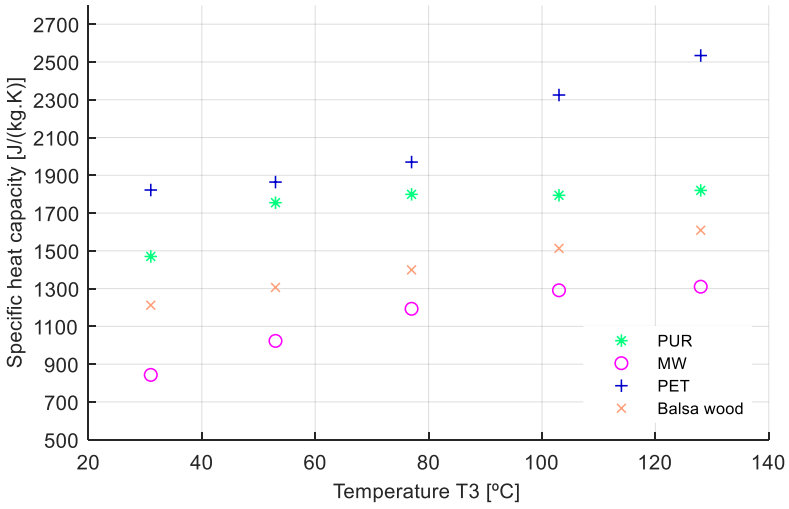

Figure 3.12. Specific heat capacity/temperature_T3 register.

It can be seen that balsa wood seems to be the material for which the heat capacity is less affected by the variation of the temperature. According to the literature (Forest Products Laboratory, 2010), the heat capacity of wood is practically independent of density or species, although it depends on the temperature. That dependency can be estimated (for dry wood), according to (Forest Products Laboratory, 2010), by the following formula (considering temperature in K):

$$cp\ [J/(kg.K)] = (0.1031 + 0.003867\ T) \times 1000 \quad (3.2)$$

The specific heat capacity results for balsa are consistent with the results obtained using expression (3.2), varying 5% at the most.

The polymeric foams seem to be more influenced by temperature, being PET foam the one most affected. Although PET and MW presented a similar behaviour in what concerns to the influence of temperature in the thermal conductivity values, in the case of specific heat this was not true. Mineral wool has the lowest specific heat out of the four materials.

4. MECHANICAL CHARACTERISATION

4.1. Experimental methodology

In technological applications, the proper determination of the elastic modulus is very important since it establishes the input for structural calculus in engineering design.

Different experimental methods can be used to obtain the elastic constants with the most commonly applied classified as static or dynamic.

The static techniques, in their different forms, are probably the most frequently used procedures. When performing these techniques, the specimens have larger dimensions, which is an advantage since it allows the results to be more representative. However, these tests are harder to perform with temperature control, given the dimensions and the requirements of the equipment.

In the present study, the determination of Young's Modulus is accomplished by an impulse excitation technique (IET). The IET is a non-destructive technique that enables fast measurements. From the experimental point of view, it is simple to implement, and some authors attribute to it greater accuracy (Lord and Morrell, 2004). This technique makes use of the resonant frequency associated with the first flexural eigenmode.

The test follows the ASTM standard E 1876 – 01 and consists in measuring the fundamental resonant frequency of the test specimens. These specimens have a suitable geometry, normally a parallelepiped bar, and are excited mechanically by a singular impact generated by an impulsive tool. A transducer, in this case, a piezoelectric sensor, detects the resulting mechanical vibrations of the specimen and transforms them into electric signals. Specimen supports, impact locations, and signal pick-up points are selected to induce and measure the first eigenmode of the test specimen. The signals are analysed, and the fundamental resonant frequency is determined.

The elastic modulus, for a parallelepipedal test specimen, is determined according to equation 4.1.

$$E = 0{,}9465\left(\frac{m{f_f}^2}{w}\right)\left(\frac{L^3}{t^3}\right)T_1 \quad (4.1)$$

where:

m – specimen mass, (g);

f_f – Resonance frequency in bending (Hz);

w – Width (mm);

L – Length (mm);

t– Thickness (mm);

T_1- Correction factor for fundamental flexural mode to account for the thickness and length of the test specimen, Poisson's ratio.

$$T_1 = 1 + 6.585(1 + 0.0752\mu + 0.8109\mu^2)\left(\frac{t}{L}\right)^2 - 0.868\left(\frac{t}{L}\right)^4 - \left[\frac{8.340(1+0.2023\mu+2.173\mu^2)\left(\frac{t}{L}\right)^4}{1.000+6.338(1+0.1408\mu+1.536\mu^2)\left(\frac{t}{L}\right)^2}\right] \quad (4.2)$$

where:

μ – Poisson's ratio

If $\frac{L}{t} \geq 20$, T_1 can be simplified:

$$T_1 = \left[1.000 + 6.585\left(\frac{t}{L}\right)^2\right] \quad (4.3)$$

To understand how the Young's modulus is influenced by temperature, tests were performed for different temperature conditions. Figure 4.1 shows the equipment and the test configuration.

The specimen is excited with a metallic sphere with a diameter of 3 mm, which is introduced in the oven with a guiding tube, that strikes the specimen suspended in a support. The specimen has a bonded piezometric sensor which detects the resulting mechanical vibrations. Balsa, polyethylene terephthalate (PET) rigid foam and polyurethane (PUR) rigid foam were subjected to different levels of temperature, as shown in the Table 4.1. The tests for polymeric materials were only carried out for temperatures up to 100ºC, since this type of material starts to degrade at approximately this temperature. Testing

of these materials was performed with small increments in the increase of temperature, to ascertain if the glass temperature, Tg, could be identified as being related to the decrease of the elastic modulus. Balsa, on other hand, can withstand more temperature and, for this reason, the tests were performed up to the maximum temperature allowed by the equipment, 160 ºC. At least three tests were performed at each temperature level.

Table 4.1. Temperature levels of the IET tests

Balsa	40ºC; 80ºC; 120ºC; 160ºC
Polymeric foams (PET and PUR)	30ºC; 40ºC; 50ºC; 60ºC; 70ºC; 80ºC; 90ºC; 100ºC;

,

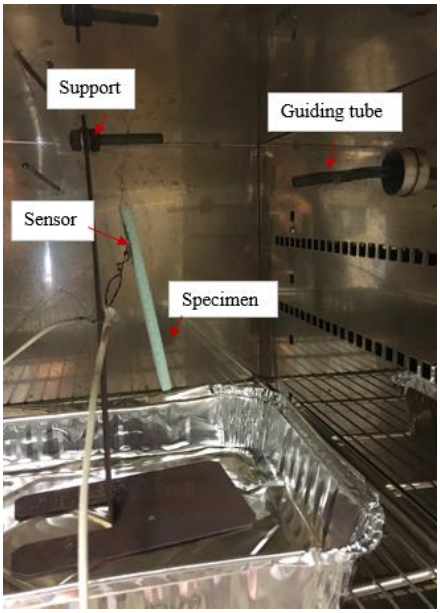

Figure 4.1. IET test configuration.

To validate the technique a well-known material, stainless steel AISI 316, was tested. Then, PET foam, PUR foam, and balsa wood specimens were tested. Mineral wool was excluded from this test because this technique is not suitable for testing these kinds of materials. Given the small dimensions of the specimens, it is not possible to cut parallelepiped shaped samples of mineral wool. As for the PET foam, due to the anisotropy, generated by the production process, specimens were cut in two directions. The specimens

cut in the longitudinal direction were labelled PET-L, and in transversal PET-T. Small holes were created close to one of the extremities of the test specimens to allow them to be supported during the test, see Figures 4.2 to 4.4.

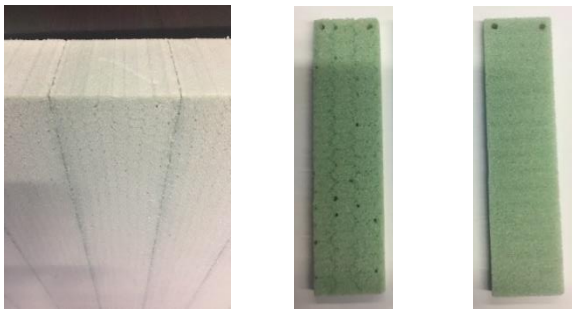

a) b) c)

Figure 4.2. IET specimens: a) PET sample; b) PET Specimen - Longitudinal direction (PET-L); c) PET Specimen – Transversal direction (PET-T).

The PUR foam is an isotropic material and thus the test specimens were cut without a specific direction (see Figure 4.3).

a) b)

Figure 4.3. IET specimens: a) PUR sample; b) PUR Specimen.

Balsa, as a type of wood, is an orthotropic material and thus exhibits independent mechanical properties according to the chosen direction. Test specimens were extracted from a Balsa beam across the longitudinal axis *L* (direction of the fibre grain), parallel to the grain (0º, labelled BAL-L0) and the tangential axis *T* (labelled BAL-T) (see Figure 4.4).

a) b) c)

Figure 4.4. IET Specimens: a) Balsa wood sample; b) Balsa wood - Longitudinal direction 0º (BAL-L0º); c) Balsa wood - Transversal direction (BAL-T).

After impact, the response in the time domain is recorded. By applying a Fourier transform in the time domain, the response in the frequency domain is obtained (see Figure 4.5). The first peak corresponds to the first eigenmode in bending. The other peaks that may be recorded are related to higher eigenmodes.

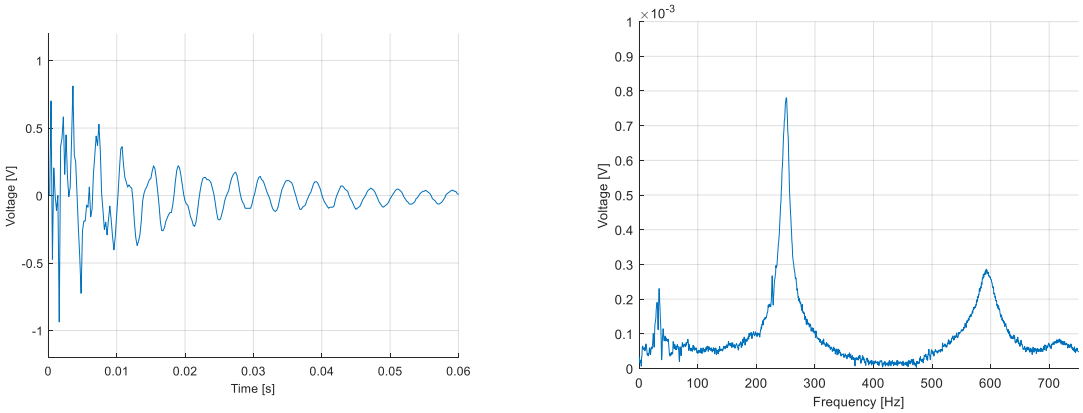

a) b)

Figure 4.5. Recorded signal obtained with the specimen PET-T at 70ºC: a) In time domain; b) In frequency domain.

4.2. Results and discussion

Table 4.2 presents the data and the results obtained for the stainless-steel specimens, at ambient conditions (23ºC and 50%). According to literature, the elastic

modulus of stainless steel AISI 316 is 187.5 GPa, 7% larger than the obtained value of 174 GPa.

Table 4.2. Data and results of IET test, for the steel specimens.

Specimen Reference	L (mm)	w (mm)	t (mm)	m (g)	f_f (Hz)	T_1	E (GPa)
S1	75,22	21,92	0,70	8,71	610,35	1,0006	174
S2	75,21	21,90	0,70	8,71	610,35	1,0006	174
S3	75,20	21,92	0,70	8,71	610,35	1,0006	174
S4	75,20	21,93	0,70	8,71	610,35	1,0006	174
S5	75,22	21,90	0,70	8,71	610,35	1,0006	174
Mean ± sd	75,21 ± 0,01	21,91 ± 0,01	0,7 ± 0,00	8,71 ± 0,00	610,35 ± 0,00	1 ± 0,00	174 ± 0,16

Table 4.3 lists the core materials specimens' physical characteristics. The two balsa specimens were not cut from the same wood sample, and for this reason, the density of the specimens present significant variation. The balsa longitudinal specimen was cut from a thin slat (2 mm). A thicker slat (20 mm) was used to cut a slice in the transversal direction.

Table 4.3. Balsa, PUR and PET test specimens' physical characteristics.

Specimen:	Balsa Longitudinal direction 0º (BAL-L0º)	Balsa Transversal direction (BAL-T)	PUR (PUR)	PET Longitudinal direction (PET-L)	PET Transversal direction (PET-T)
m (g)	0.8672	0.9583	0.6153	1.1736	1.1507
L (mm)	99.20	100.09	100.78	99.24	99.92
w (mm)	25.22	20.18	25.19	24.90	24.79
t (mm)	2.21	4.85	4.94	5.45	5.35
L/t	44.96	20.65	20.41	18.21	18.69
T_1	1.0033	1.0154	1.0157	1.0198	1.0188
Density (kg/m^3)	157	98	49	87	87

The IET results of the balsa wood specimens for different temperature levels are presented in Table 4.4. As can be seen, there is a slight increase in the value of the elastic modulus at 40ºC, possibly due to a reduction of humidity presented in the wood fibres. However, the tendency of the elastic modulus is to decrease with temperature. This reduction was noticed in both the longitudinal direction (parallel to the grain) and in the transversal direction. The difference of the elastic modulus obtained for the longitudinal direction (parallel to the grain) is very large when compared with the transversal direction, evidencing the large anisotropy assigned to the balsa wood. That difference can be magnified by the density differences, since the specimen in the longitudinal direction was considerably denser.

In order to understand how density could enhance this difference, another test was performed, at ambient conditions, for a specimen with larger dimensions and with a density closer to that of the transversal direction specimen (86 kg/m^3)), see Figure 4.6.

Figure 4.6. IET test configuration for bigger specimen's dimensions.

The value obtained for the Young's modulus was 1.08 GPa, 21% lower than 1.37 GPa (value obtained at ambient conditions for the specimen with a density of 157 kg/m^3). Comparing that value with the Young modulus for the transversal direction, 19.4 MPa the difference is still very large. However, the obtained relation between longitudinal and transversal modulus, (E_T/E_L) is approximately 0.018, which is in accordance with relations presented for balsa in the literature (0.015), according to (Forest Products Laboratory, 2010).

Table 4.4. Variation of the elastic modulus of the balsa wood with temperature (mean values and standard deviation).

Balsa Wood Specimens	**Longitudinal direction 0º (BAL-L0º)**		**Transversal direction (BAL-T)**	
	f_f (Hz)	**E (GPa)**	**f_f (Hz)**	**E (MPa)**
23ºC	679.78 ± 0.00	1.37 ± 0.00	219.56 ± 0.00	19.38 ± 0.00
40ºC	692.85 ± 11.52	1.42 ± 0.05	229.74 ± 0.17	21.22 ± 0.03
60 ºC	680.51 ± 1.69	1.37 ± 0.01	216.53 ± 5.77	18.86 ± 1.00
80 ºC	679.59 ± 0.01	1.37 ± 0.00	209.86 ± 0.02	17.7 ± 0.00
100 ºC	679.57 ± 0.03	1.37 ± 0.00	203.16 ± 5.81	16.6 ± 0.96
120 ºC	672.9 ± 11.52	1.34 ± 0.05	199.87 ± 0.01	16.06 ± 0.00
140 ºC	666.22 ± 11.58	1.32 ± 0.05	196.53 ± 5.76	15.54 ± 0.90
160 ºC	659.6 ± 0.00	1.29 ± 0.00	189.86 ± 0.02	14.49 ± 0.00
24 h after	699.85 ± 0.02	1.45 ± 0.00	228.54 ± 0.10	20.4 ± 0.80

The tests were repeated after cooling (24 hours later) and the elastic modulus had recovered the value obtained at 40ºC.

The IET results of the PET and PUR for different temperature levels are presented in Tables 4.5 and 4.6, respectively.

As can be seen, the temperature has a bigger influence in polymeric materials, particularly in PET. For the transversal direction at 100ºC, the reduction of elastic modulus was 62%, when compared to that registered at ambient conditions, while for the longitudinal direction the reduction was 10% shorter. PUR presents a reduction of approximately 34% for the same temperatures.

As for the balsa wood, the tests were repeated after cooling (24 hours later) and all of the materials presented an increase of the elastic modulus when compared with the initial tests at 23ºC.

Table 4.5. Variation of the elastic modulus of the PET with temperature (mean values and standard deviation).

PET foam Specimens	Longitudinal direction (PET-L)		Transversal direction (PET-T)	
	ff (Hz)	E (MPa)	ff (Hz)	E (MPa)
23ºC	264.06 ± 1.76	20.37 ± 0.27	262.03 ± 0.00	18.86 ± 0.00
30ºC	258.99 ± 3.05	19.6 ± 0.46	262.03 ± 0.00	18.86 ± 0.00
40ºC	255.94 ± 0.00	19.14 ± 0.00	262.03 ± 0.00	18.86 ± 0.00
50ºC	254.92 ± 1.76	18.99 ± 0.26	262.03 ± 0.00	18.86 ± 0.00
60ºC	249.84 ± 0.00	18.23 ± 0.00	260 ± 1.76	18.57 ± 0.25
70ºC	231.56 ± 0.00	15.66 ± 0.00	251.64 ± 1.09	17.39 ± 0.15
80ºC	219.38 ± 0.00	14.06 ± 0.00	240.17 ± 0.00	15.84 ± 0.00
90ºC	167.67 ± 0.16	8.21 ± 0.02	215.9 ± 3.42	12.81 ± 0.40
100ºC	162.5 ± 3.52	7.72 ± 0.33	181.35 ± 0.00	9.03 ± 0.00
24h after	280.31 ± 0	22.95 ± 0	274.15 ± 0.35	20.64 ± 0.05

Table 4.6. Variation of the elastic modulus of the PUR with temperature (mean values and standard deviation)

PUR foam Specimens	PUR foam	
	f_f (Hz)	E (MPa)
23ºC	261.83 ± 2.39	13.7 ± 0.25
30ºC	257.7 ± 2.23	13.27 ± 0.23
40ºC	251.97 ± 1.74	12.69 ± 0.18
50ºC	247.39 ± 1.68	12.23 ± 0.17
60ºC	240.58 ± 1.68	11.56 ± 0.16
70ºC	235.29 ± 0.53	11.06 ± 0.05
80ºC	227.46 ± 0.70	10.34 ± 0.06
90ºC	218.51 ± 2.64	9.54 ± 0.23
100ºC	213.11 ± 0.64	9.07 ± 0.05
24h after	260 ± 0.31	13.51 ± 0.03

The elastic Young's modulus was also determined by performing bending tests (static technique). Bending tests were conducted by placing a beam of material across a span and pushing it down along the span, bending it until failure. These tests can be designated as 3- point bending tests or 4-point bending tests. The 3-point description comes from the two points of support at the ends of the material and the one point of deflection brought down to the middle of the material. The 4-point bending tests are conducted similarly to 3-point bending tests except that rather than one-point source being brought down to the centre of the span, two points slightly separated from the centre are brought down in contact with the material. This separation of the two-point sources spreads the region of bending out from the centre such that a larger portion of the material is sustaining the maximal strain when compared to one point of deflection.

Figure 4.7 presents the 4-point bending test configuration. The tests were performed using a universal testing machine Shimadzo, equipped with a load cell of 100 kN. The universal testing machine was not equipped with an oven or a climatic chamber: thus, the bending tests were only performed at ambient conditions (23ºC and 50%HR).

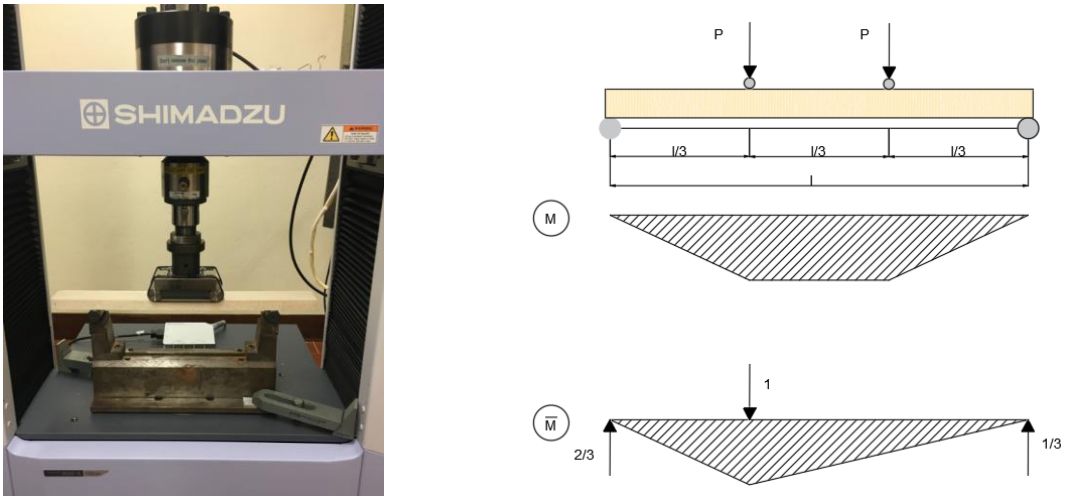

a) b)

Figure 4.7. Bending test configuration – 4-point bending: a) Photographic register of the test configuration; b) Scheme of test - bending diagrams: due to the load test configuration (M) and due to a unitary load ($\bar{M}$).

The displacement considered was measured through the machine, corresponding to the displacement of the load rollers. This displacement contains not only the deformations due to the bending but also the indentation of the rollers.

In order to determine the contribution of the rollers indentation on the displacement register, an additional test was carried out to quantify the indentation effect. This test consisted in use the same test configuration (4-point bending test) but with the specimen supported in a rigid base. Considering the displacement readings on the rollers, it was possible to determine the corrected displacement, by subtracting the compliance (of the indentation test) multiplied by the load register (bending test), to the bending test displacement, see equation 4.4.

$$\delta_{cor} = \delta - \frac{1}{k}P \tag{4.4}$$

where:

δ_{cor} - Corrected displacement (mm);

δ – Displacement measured during the bending test (mm);

k – Rigidity measured during the indentation test (N/mm);

P – Load measured during the bending test (N);

Figure 4.8 presents the load/displacement graph of the test specimens. Only one test proceeded until failure. The other two specimens were stopped at a defined displacement.

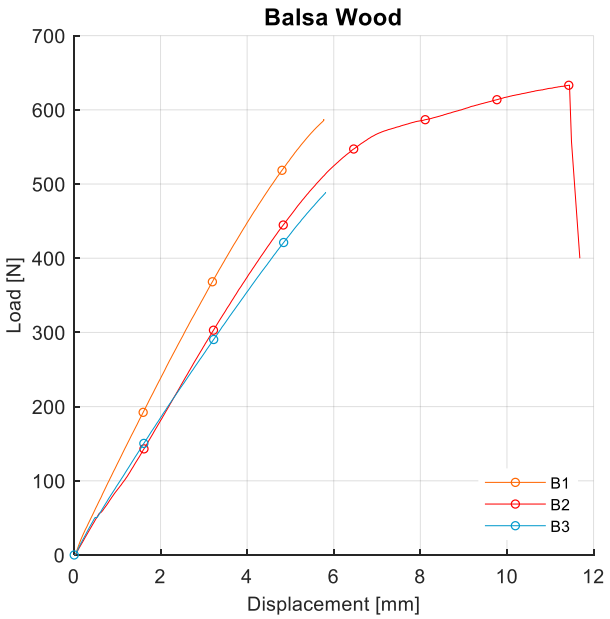

Figure 4.8. Load/displacement curves – bending tests.

Disregarding the contribution of shear, the deflection is givening by the following equation, deduced for the position at l/3, see Figure 4.7b). The test span was 330 mm.

$$\delta = \int \frac{M\bar{M}}{EI} dx = \frac{5Pl^3}{162EI} \quad (4.5)$$

where:

M - bending moment (N.m)

$\bar{M}$ - Bending moment due to a unitary load (N.m)

P – Test load (N);

l – Test span (m);

E – Young's modulus (Pa);

I – Inertia of the bending section (m^4);

The elastic modulus is then determined by the linear part of the slope of the load/displacement graph, multiplied by $\frac{5l^3}{27bh^3}$, see equation (4.6):

$$E = \frac{P}{2\delta} \times \frac{5l^3}{162 \times \frac{bh^3}{12}} = \frac{P}{\delta} \frac{5l^3}{27bh^3} \quad (4.6)$$

Table 4.7 presents the data and results of the Young's modulus of the balsa wood bending tests. These test specimens, BAL-1, BAL-2 and BAL-3 were cut from the same balsa wood sample.

Table 4.7. Data and Young's modulus of balsa wood specimens.

Balsa wood	**Length (mm)**	**Width (mm)**	**Thickness (mm)**	**Mass (g)**	**Density (kg/m^3)**	$\frac{P}{\delta}$	**E (GPa)**
BAL-1	480.5	48.72	20.38	52,05	109	114.45	1.85
BAL-2	480.0	48.60	20.20	48,49	103	100.62	1.67
BAL-3	480.3	48.74	20.37	45,62	96	90.16	1.46
Mean ± sd	480.23 ± 0.25	48.7 ± 0.1	20.3 ± 0.1	48.7 ± 3.2	102 ± 12	107.4 ± 12.8	1.66 ± 0.20

The bending elastic modulus of balsa wood, according to (Forest Products Laboratory, 2010), is 3.4 GPa for a specific density of 0.16 (160 kg/m^3) and with 12% of moisture. Silva and Kyriakides, (2007) also presented elastic modulus for several densities of balsa wood, 0.61 GPa, 1.99 GPa and 3.04 GPa, corresponding to densities of 65 kg/m^3, 120 kg/m^3, and 146 kg/m^3, respectively. Taking this into account, both results (IET and 4-point bending test) are in accordance with the literature.

The mean value of the elastic modulus obtained from the bending of balsa wood, 1.66 GPa, is 35% greater than the value obtained from the IET results, (at ambient conditions), 1.08 GPa, for a similar density. This stiffness increase can be related to the wood fibres, which in the static test the tensile resistance can be mobilized more effectively. Although, there is another reason for this to occur, as the contribution of shear for failure in bending may be being neglected. According to ASTM C 939-00, a good rule of thumb for the four-point bending test is that the span length divided by the thickness should be greater than 20, and in this case, this relation is below 20 (16), meaning that the shear contribution cannot be totally dismissed. The test until failure allowed the determination of the shear strength, τ, once the specimen failure registered is by shear, see Figure 4.9.

The shear strength can be determined by the following equation:

$$\tau = \frac{3T}{2hb} \qquad (4.7)$$

where:

T – Shear load (N);

h - Height (mm);

b – Width (mm).

Table 4.8 presents the result from the shear strength of balsa wood.

Table 4.8. Result from the shear strength of balsa wood.

Balsa wood	b (mm)	h (mm)	Maximal test load (N)	T (N)	τ (kPa)
BAL -2	48.60	20.20	587	293.5	444

Figure 4.9. Photographic register of the specimen BAL-2.

The shear strength can also be determined by subjecting the test specimen to shear stress by applying two parallel and opposite forces, see Figure 4.10. The shear strength is defined as the ratio of the maximum force of the test, F_m, which causes failure along a plane parallel to the direction of the applied forces, to the area of the plane on which the force acts.

$$\tau = \frac{F_m}{bl} \quad (4.8)$$

where:

F_m – Maximum force (N);

l - Length (mm);

b – Width (mm).

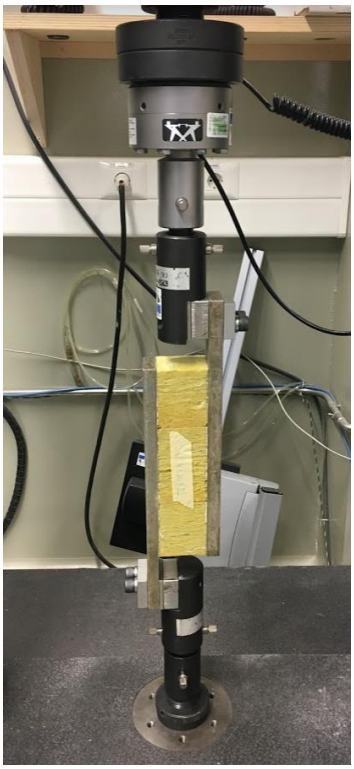

Figure 4.10. Photographic register of the test configuration.

In order to determine the shear strength along the main surfaces, the specimen was subjected to a traction load at a constant rate of 3 ± 0.5 mm/min, using rigid supports bonded to the material. The corresponding load–displacement curve was obtained. Each sample consisted of three test specimens with nominal dimensions of 250 mm x50 mm.

Tests specimens of polyethylene terephthalate (PET) rigid foam, polyurethane (PUR) rigid foam, and mineral wool were prepared. For the PET foam and mineral wool specimens, different directions were considered (longitudinal and transversal), see Figure 4.11. Additionally, for the PET foam, a supplement set of specimens in transversal direction was considered, contemplating glue lines, labelled as PET foam TG, (T from transversal and G from glue). The shear force-strain curves are presented in Figure 4.12.

This method is used for thermal insulation materials, EN 12090 (2013), normally not very resistant to shear, when compared for instance with balsa wood. The procedure is not suitable for wood because failure, in this case, would occur in the bonding between the material under study and the rigid plates, thus not obtaining the material's resistance.

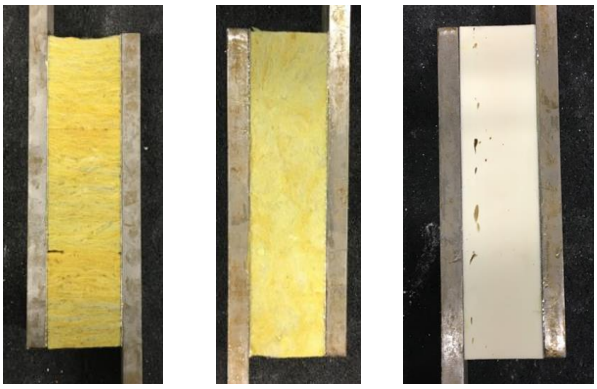

a) b) c)

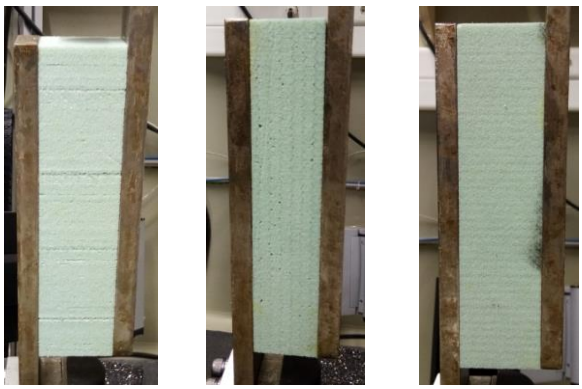

d) e) f)

Figure 4.11. Test specimens: a) Mineral wool (direction 1); b) Mineral wool (direction 2); c) PUR foam; d) PET foam (transversal direction with glue lines); e) PET foam (longitudinal direction); f) PET foam (transversal direction).

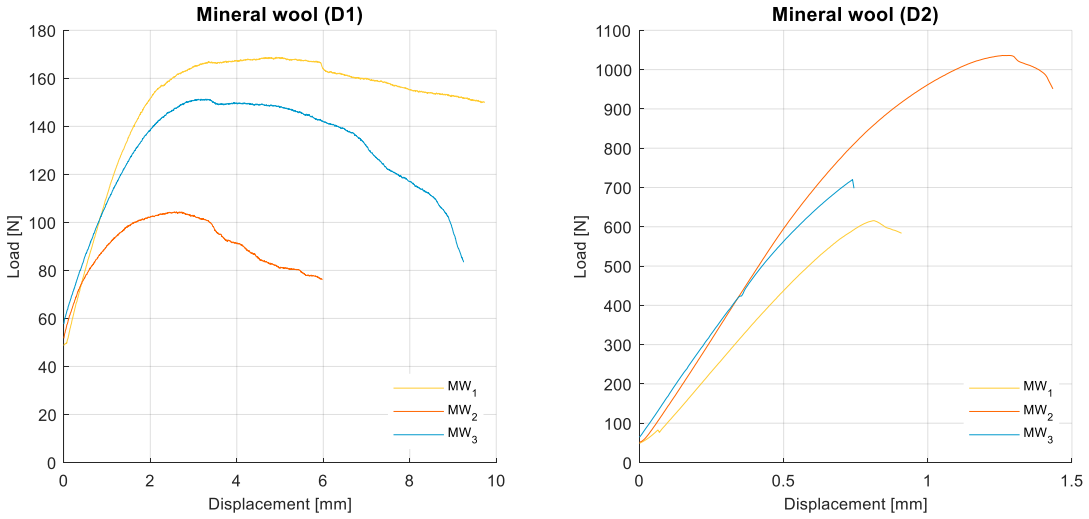

a) b)

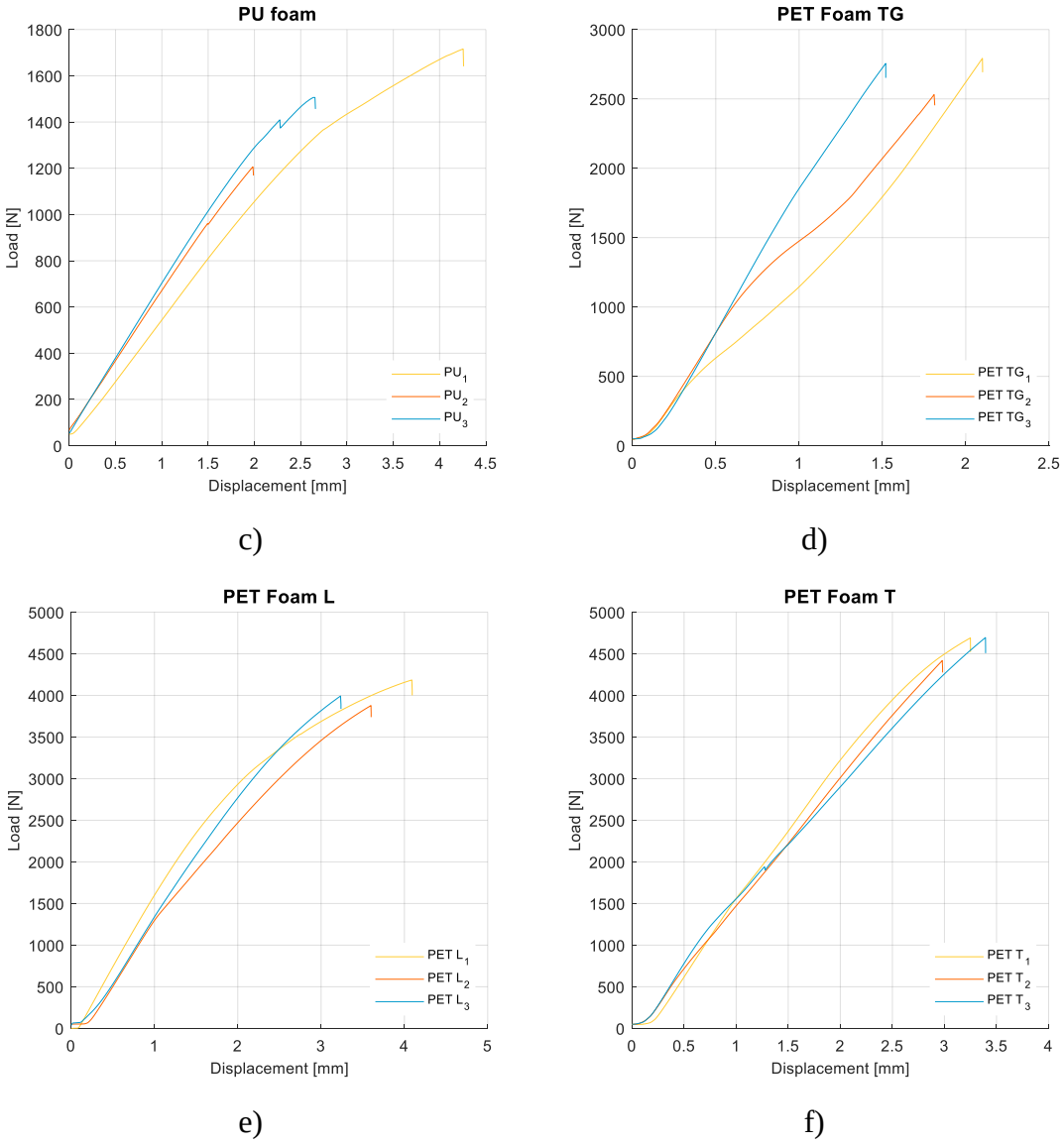

Figure 4.12. Shear force-strain curves; a) Mineral wool (direction 1 – D1); b) Mineral wool (direction 2 – D2); c) PUR foam; d) PET foam (transversal direction with glue lines); e) PET foam (longitudinal direction); f) PET foam (transversal direction).

Table 4.9 presents the results from the shear strength. As can be seen, the fibre direction has a big influence for the mineral wool shear strength. Relative to the PET foam, the glue lines do not increase the shear resistance, as the results show the highest shear strength of all (not considering balsa) for the PET transversal direction without the glue lines.

Table 4.9: Result from the shear strength of the remaining materials (mean values and standard deviation).

Material	Maximal load (N)	Shear strength (kPa)
Mineral wool (D1)	161 ± 9	13 ± 1
Mineral wool (D2)	791 ± 219	63 ± 18
PUR foam	1404 ± 172	112 ± 14
PET foam TG	2693 ± 142	215 ± 11
PET foam L	3909 ± 100	313 ± 8
PET foam T	4601 ± 158	368 ± 13

Compression tests were additionally preformed for all types of core materials, balsa, PUR foam, PET foam, and mineral wool, see Figure 4.13.

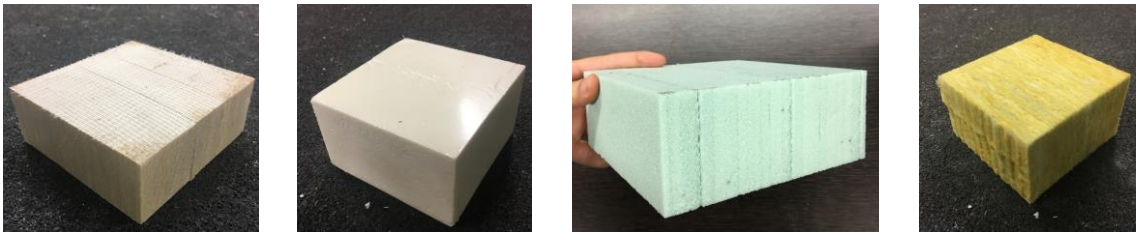

a) b) c) d)

Figure 4.13. Photographic register of the specimens after compression test: a) Balsa wood; b) PUR foam; c) PET foam; d) Mineral wool.

All specimens were cut to nominal dimension of 100 x 100 from commercially available panels, except for the balsa wood specimens. The balsa wood panels were by juxtaposing cubes. They were kept together by a meshed bonded to one of the sides. To performed the compression tests, it was first necessary to bond the cubes to each other using a white wood glue. Figure 4.14 illustrates the preparation of these balsa wood specimens.

a)

b)

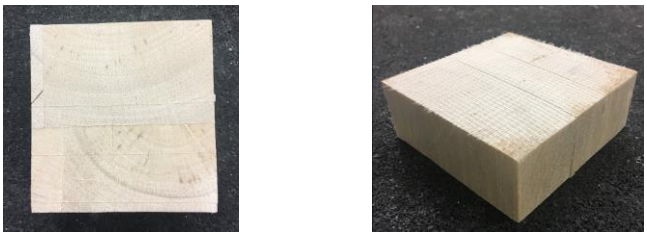

c)

Figure 4.14. Photographic record of the balsa panel bonding: a) Glue application; b) Panel after polishing; c) Specimens cut from the panel.

The test consisted in applying a compressive load at a constant rate (thickness/10, in mm/min) as established in the EN 826 (2013) standard, until 50% strain was achieved, see Figure 4.15. The tests were performed using an electromechanical universal testing machine, INSTRON 5884, with a load cell of 150 kN for the balsa wood specimens and of 30 kN for the other specimens.

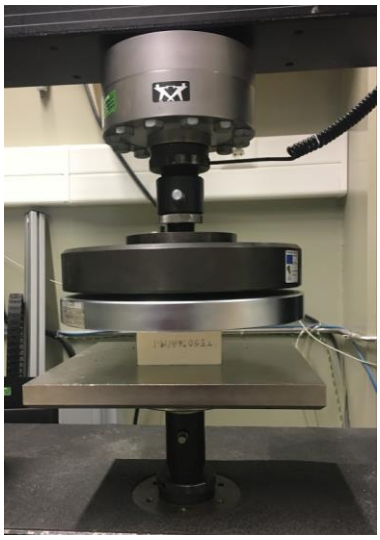

Figure 4.15. Compression test configuration.

Table 4.10 presents the results of the compression tests. The compression load-extension curves are presented in Figure 4.16. The tests were carried out until reaching 50% of the extension, to see the material's behaviour at higher deformations. The maximal load considered to calculate the compressive strength corresponds to the first peak, for all materials tested. In the case of the PUR foam, for instance, the specimens had a peak (around 10% extension), and then the material presented an increase of load, (after a slight decrease). Also, mineral wool and PET foam specimens presented an increase after the initial peak, having reached that at 50% of extension with a similar or even superior load value.

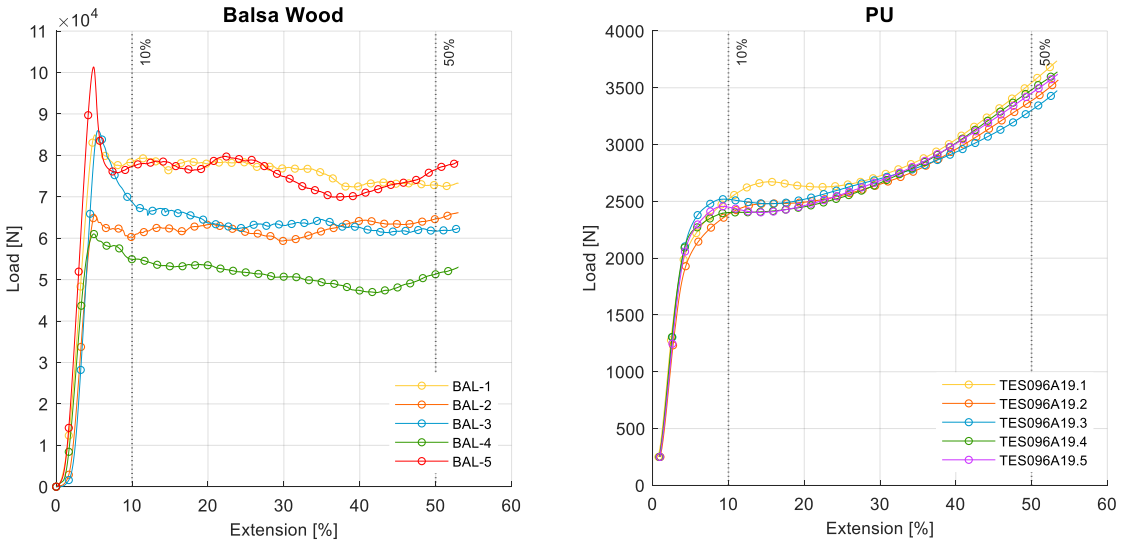

a) b)

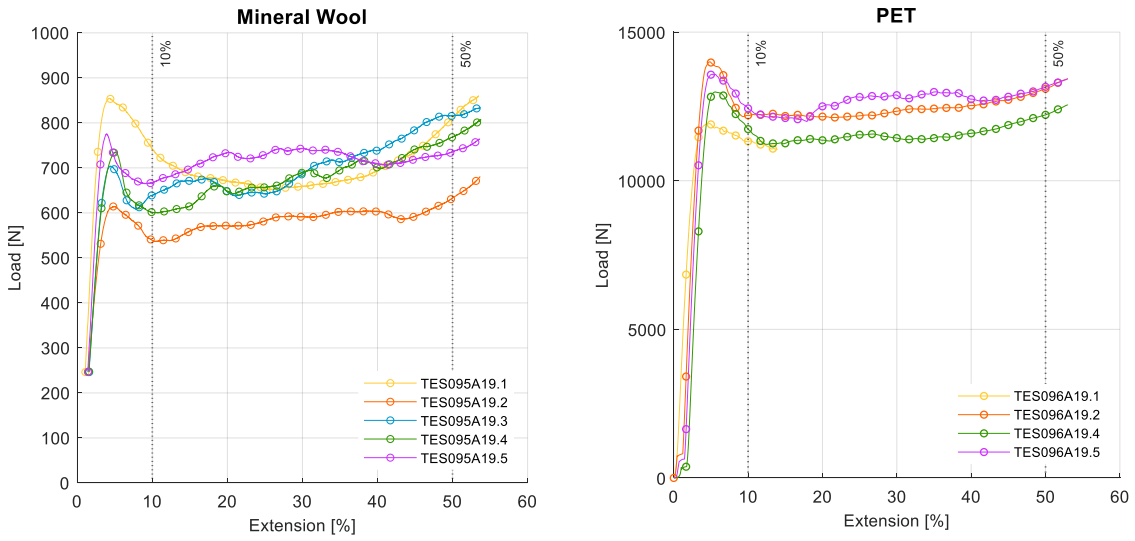

c) d)

Figure 4.16. Compression tests results: a) Balsa wood; b) PUR foam; c) Mineral wool; d) PET foam.

Table 4.10. Compression test results (mean values and standard deviation).

Material	Specimen	Maximal load (N)	Compressive strength (kPa)
Mineral Wool		792 ± 70	79 ± 7
PUR foam		2507 ± 102	252 ± 11
Balsa		79891 ± 16340	8066 ± 1673
PET foam		13212 ± 807	2181 ± 135

Figure 4.17 presents a photographic record of the compression test specimens during and after testing.

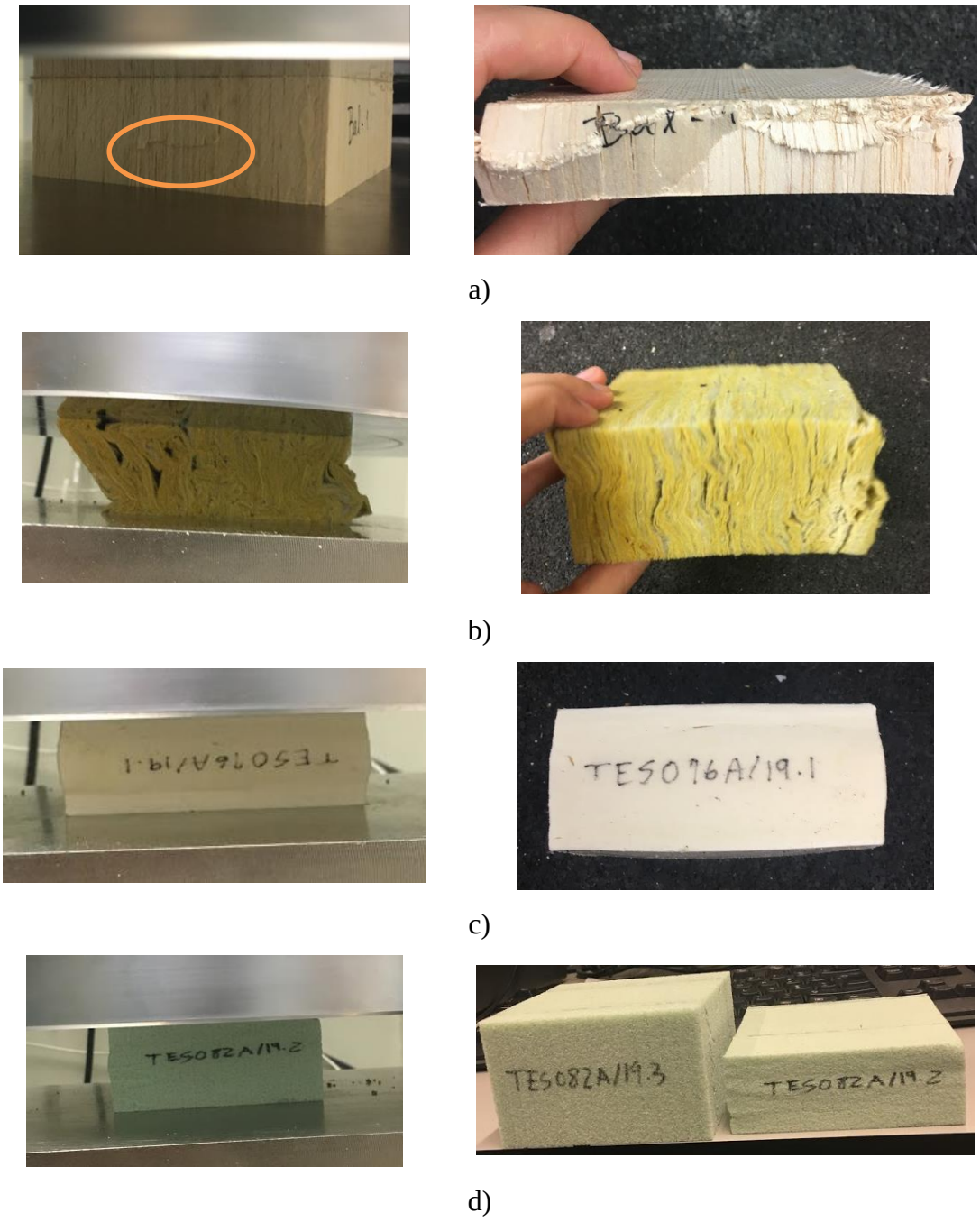

Figure 4.17. Photographic register of the **c**ompression test specimens': a) Balsa wood; b) Mineral Wool; c) PUR foam; d) PET foam.

5. CONCLUSIONS

From a design standpoint, it is particularly important to obtain an adequate understanding on how the mechanical and thermal properties of materials are affected in-service temperatures.

In this work, Balsa wood, polyethylene terephthalate (PET) and polyurethane (PUR) rigid foams, and mineral wool panels (MW), frequently used in the core of climatic chamber walls, were studied thermally and mechanically.

Regarding the thermal characterisation, it can be concluded that the developed experimental setup allowed to perform tests in similar conditions of real applications. The results obtained with this set up were validated with standardised tests used to evaluate the thermal conductivity at low temperature.

In all cases, the thermal conductivity increased with temperature. This relation appeared to be linear for all of the tested materials, except for balsa wood, which showed a non-linear behaviour. Both foams under study presented a leap in thermal conductivity for higher temperatures. This increase is possibly related to the glass-transition temperature of the original polymers. After testing, it was possible to see that the PUR foam was substantial degraded due to high temperature exposure. The thermal conductivity of the mineral wool and the PET foam presented a very similar behaviour and performance.

The specific heat results were found to be similar to those found in the literature. The polymeric foams seem to be more influenced by the temperature, for which the PET foam was the most affected. Mineral wool has the lowest specific heat of the four materials.

Regarding the mechanical characterisation, it is important to understand how the mechanical properties of the core materials in the sandwich panels changed when subjected to a wide range of temperatures. In this context, this work used the impulse excitation technique (IET) to evaluate the variation of the Young's modulus with temperature. The results showed that the tendency of the elastic modulus is to decrease with temperature. It was verified that temperature had a bigger influence in the polymeric materials, particularly for the PET. However, the tests (for polymeric foams and balsa) were repeated after cooling

(24 hours later) and all of the materials presented an increase of the elastic modulus when compared with the initial tests at 23ºC, possibly due to a reduction of moisture. Other mechanical tests were performed (without temperature variation) in order to complement the mechanical characterisation.

The application of IET to determine the elastic modulus seems to be a feasible alternative to perform static tests that would require the installation of universal testing machines inside climatic chambers.

5.1. Future work

The evaluation of the mechanical and thermal behaviour of MW, PUR, PET and Balsa wood sandwich panels carried out in this thesis has shown that their behaviour change markedly with temperature. Although it is considered that the main objectives of this work have been achieved, some future work that may be considered would include:

- to evaluate the performance of these materials when subjected to the simultaneous variation of temperature and moisture content;
- to study the effect of aging of these materials (namely after submitting to freeze/thaw cycles).

REFERENCES

Zenkert, D. (1995), "An introduction to sandwich construction", Engineering Materials Advisory Services, Sheffield.

Avó de Almeida, M.I. (2009). "Comportamento estrutural de painéis sanduíche compósitos para aplicações na indústria da construção". Tese de Mestrado em Engenharia Civil, Instituto Superior Técnico, Universidade Técnica de Lisboa, Lisboa.

Davies, J.M. (2001), "Lightweight Sandwich Construction", Oxford Blackwell Science Lta, Oxford.

Econcore (2020), "Sandwich technology ". Accessed at 24 of february of 2020, in http://www.econcore.com/en/technology/sandwich-technology

Sivertsen, K. (2007), "POLYMER FOAMS", 3.063 Polymer Physics, Spring.

Sorrentino, L., Di Maio, E., Iannace, S. (2010), "Poly(ethylene terephthalate) foams: correlation between the polymer properties and the foaming process", Journal of Applied Polymer Science, 116, 27-35.

Garrido, M., Correia, J., Keller, T. (2015), "Effects of elevated temperature on the shear response of PET and PUR foams used in composite sandwich panels", Construction and Building Materials, 76, 150-157.

Smithers (2014), "Polymer Foams Market Expected to Consume 25.3 Million Tonnes by 2019". Accessed at 23 of June of 2020, in, http://www.smithersrapra.com/news/2014/may/polymer-foam-market-toconsume-25-3-million-tonnes.Borrega, M., Gibson, L. (2015), "Mechanics of balsa (Ochroma pyramidale) wood", Mechanics of Materials, 84, 75–90.

Forest Products Laboratory. (2010), "Wood handbook - Wood as an engineering Material", General Technical Report FPL-GTR-190. Madison, WI: U.S. Department of Agriculture, Forest Service, Forest Products Laboratory.

Borrega, M., Ahvenainen, P., Serimaa, R., Gibson, L. (2015), "Composition and structure of balsa (Ochroma pyramidale) wood", Wood Science and Technology, 49, 403-420.

Grenestedt, J., Bekisli, B. (2003), "Analyses and preliminary tests of a balsa sandwich core with improved shear properties", International Journal of Mechanical Sciences, 45, 1327–1346.

Huiyuan, S., Weiqing, L., Fang, H. (2018), "Damage characteristics analysis of GFRP-Balsa sandwich beams under Four-point fatigue bending", Composites Part A: Applied Science and Manufacturing, 109, 564-577.

Li, X., Liu, W., Fang, H., Huo, F., Wu, P. (2019), "Flexural creep behavior and life prediction of GFRP-balsa sandwich beams", Composite Structures, 224, 111009.

Osei-Antwi, M., Castro, J., Vassilopoulos, A., Keller, T. (2013), "Shear mechanical characterization of balsa wood as core material of composite sandwich panels", Construction and Building Materials, 41, 231–238.

Silva, A., Kyriakides, S. (2007), "Compressive response and failure of balsa wood", International Journal of Solids and Structures, 44, 8685–8717.

Mima (2020)," What is mineral wool?". Accessed at 23 of June of 2020, in, http://mima.info/about-mineral-wool/

EURIMA (2006), European Insulation Manufacturers Association, www.eurima.org,

Berardi, U., Naldi, M. (2017), "The impact of the temperature dependent thermal conductivity of insulating materials on the effective building envelope performance", Energy and Buildings, 144, 262–275.

Berardi, U. (2019), "The impact of aging and environmental conditions on the effective thermal conductivity of several foam materials", Energy , 182, 777e794.

Karamanos, A., Hadiarakou, S., Papadopoulos, A.M. (2008), "The impact of temperature and moisture on the thermal performance of stone wool," Energy and Buildings, 40, 1402–1411.

Jelle, B.,P. (2011), "Traditional, state-of-the-art and future thermal building insulation materials and solutions – Properties, requirements and possibilities", Energy and Buildings 43, 2549–2563.

Sirris (2020), "Validating extreme working conditions for different industries ". Accessed at 22 of february of 2020, in https://www.sirris.be/climate-chamber-extreme-working-conditions-differentnustries?_ga=2.46122982.352838089.1582246130-1392933372.1582246130

Silva, R., Brett, M., Ferreira, A.D., Serra, C., Jesus, T., Fino, M., Tadeu, A., Mendes, J., Araújo, J., Santos, R. (2020), "Computational Fluid Dynamics Modeling and Experimental Validation of the Thermofluidic Performance of Climatic Chambers", Journal of Thermal Science and Engineering Applications, 12, 021014.

Zhang, S., Dulieu-Barton, J., M., Thomsen, O., T. (2015), The effect of temperature on the failure modes of polymer foam cored sandwich structures", Composite Structures, 121, 104–113.

Pulngern, T., Chitsamran, T., Chucheepsakul, S., Rosarpitak, V., Patcharaphun, S., N., Sombatsompop, (2016), "Effect of temperature on mechanical properties and creep responses for wood/PVC composites", Construction and Building Materials, 111, 191-198.

Vahedia, N., Wua, C., Vassilopoulos, A., Keller, T. (2016), Thermomechanical characterization of a balsa-wood-veneer structural sandwich core material at elevated temperatures", Construction and Building Materials 111, 191–198.

Goodrich, T., Stefanie N., Brian, F., Lattimer, Y., Mouritz, A. (2010), "High-temperature mechanical properties and thermal recovery of balsa wood", Journal of Wood Science, 56, 437–443.

Al-Ajlan, S. (2006), "Measurements of thermal properties of insulation materials by using transient plane source technique", Applied Thermal Engineering, 26, 2184–2191.

Asdrubali, F., D'Alessandro, F., Schiavoni, S. (2015), "A review of unconventional sustainable building insulation materials", Sustainable Materials and Technologies, 4, 1-17.

Zhang, H., Fang, W., Li, Y., Tao, W. (2017), "Experimental study of the thermal conductivity of polyurethane foams", Applied Thermal Engineering, 115, 528–538.

Huang, P., Chew,Y., Chang, W., Martin, A., Lawrence M., Latif, E., Shea A., Ormondroyd, G., Dua, H. (2018), "Heat and moisture transfer behaviour in Phyllostachys edulis(Moso bamboo) based panels", Construction and Building Materials, 166, 35–49.

EN 12664 (2001). "Thermal performance of building materials and products. Determination of thermal resistance by means of guarded hot plate and heat flow meter methods. Dry and moist products of medium and low thermal resistance". European committee for standardization.

EN 12667 (2001) “Thermal performance of building materials and products. Determination of thermal resistance by means of guarded hot plate and heat flow meter methods. Products of high and medium thermal resistance.” European committee for standardization.

Simões, I., Simões, N., Tadeu, A. (2012), "Thermal delay simulation in multilayer systems using analytical solutions". Energy and Buildings, 49, 631-639.

Lord, J., D., Morrell, R. M. (2004), “Comparison of static and dynamic methods for measuring stiffness of high modulus steels and metal composites”. Canadian Metallurgical Quarterly; 53, 292-299.

ASTM E1876-15 (2015), “Standard Test Method for Dynamic Young's Modulus, Shear Modulus, and Poisson's Ratio by Impulse Excitation of Vibration”, ASTM International, West Conshohocken, PA. International.ASTM C393-00 (2000) “Standard Test Method for Flexural Properties of Sandwich Constructions”, ASTM International, West Conshohocken, PA.

EN 12090 (2013) “Thermal insulating products for building applications - Determination of shear behaviour”. European committee for standardization.

EN 826 (2013) “Thermal insulating products for building applications - Determination of compression behaviour”. European committee for standardization.

Lambda-Messtechnik GmbH Dresden (2020), Accessed at 23 of June of 2020, in, http://www.lambda-messtechnik.de/en/thermal-conductivity-test-tool ep500e/guarded-hot-plate-apparatus-lambda-meter-ep500e-design-and function.html.

ANNEX A – OVEN DOORS ADAPTATION

Figure A.1 presents the detailed drawing of the oven adaptation.

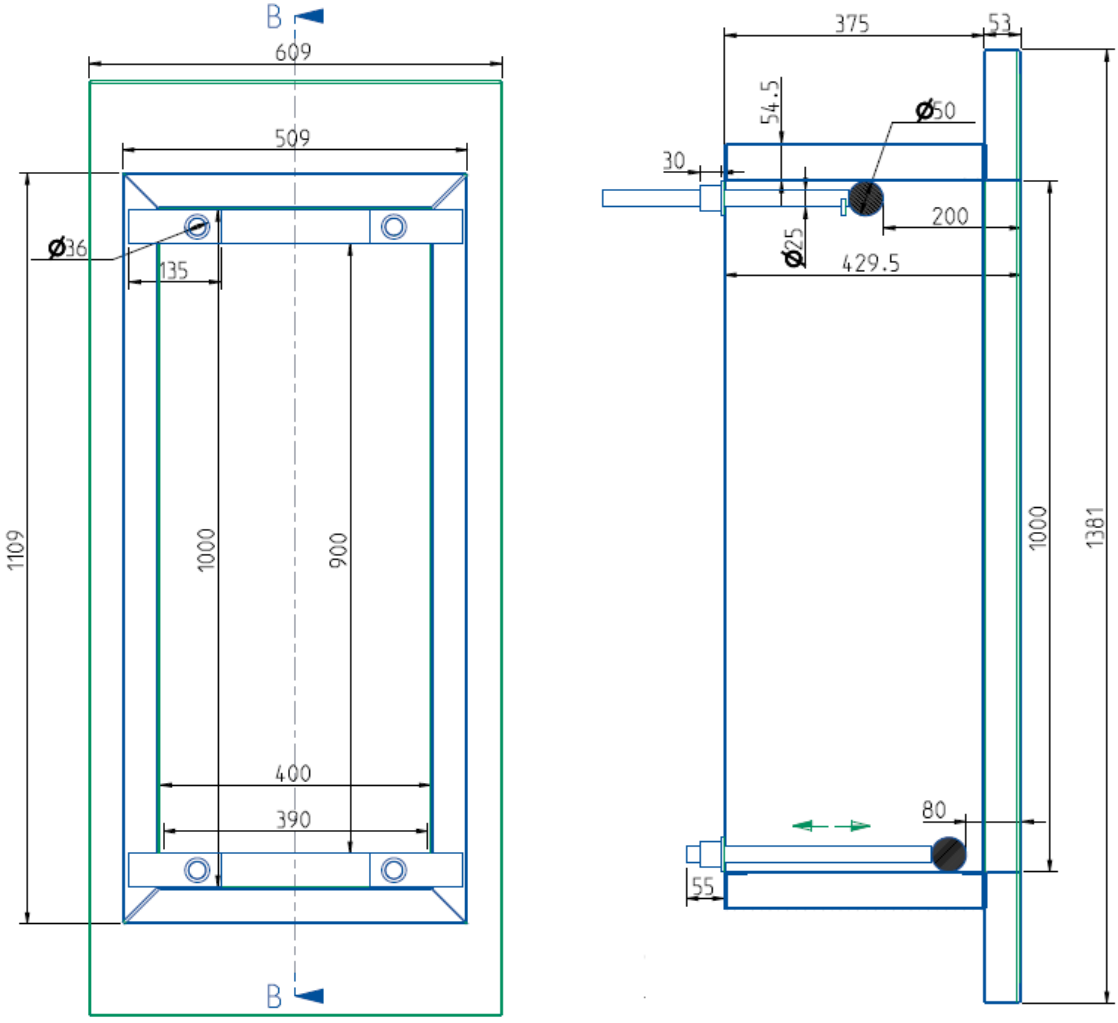

a) b)

Figure A.1. Drawing of the door adaptation: a) Frontal view; b) Side view – section B-B.

ANNEX B – THERMAL CONDUCTIVITY TEST

In order to complement the thermal conductivity study, an experimental campaign was carried out using implemented methodologies for room conditions of temperature, in this case 10ºC. For this campaign, two equipments were used, namely, a Heat Flow Meter HFM 436/3 Lambda ™ and a Guarded Hot Plate λ-Meter EP500e, see Figure B.1.

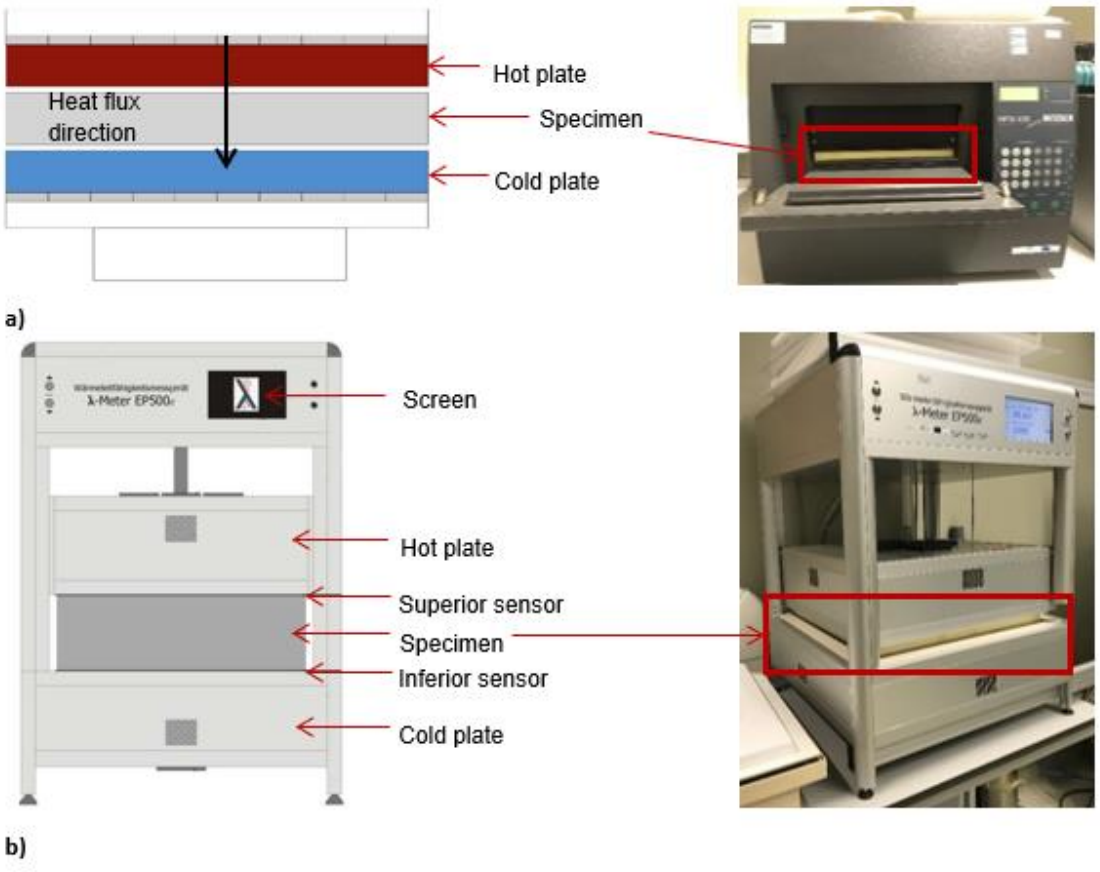

Figure B.1. Thermal conductivity equipment: a) Heat Flow Meter; b) Guarded Hot Plate (adapted from Lambda-Messtechnik GmbH Dresden, 2020).

The thermal conductivity tests of the balsa wood specimens were performed using the Guarded Hot Plate (GHP) equipment, while the thermal conductivity tests of the other materials (PET, PUR and MW) were performed using the equipment Heat Flow Meter (HFM).

For the HFM method the specimens have dimensions of 300 mm x 300 mm, and for the GHP method, the specimens have dimensions of 150 mm x 150 mm in this case it was necessary to confine the specimen with insulation material, as shown in Figure B.2.

Figure B.2. Confinement of balsa wood specimen with an insulation material.

The tests were carried out under controlled laboratory conditions of temperature and relative humidity. Balsa wood was tested in accordance with the standards EN 12667 (2001) that applies to materials with a thermal resistance not less than 0.5 m^2.K/W and the other materials were tested in accordance to EN 12664 (2001) that applies to materials with a thermal resistance not less than 0.1 m^2.K/W. Both methods establish a thermal gradient, ΔT, in equilibrium, measured by temperature sensors fixed on the plate surfaces (with different temperature) in contact with the specimen.

The equipment quantifies the steady-state heat flow through a test specimen placed between two plates with thermal sensors. The goal is to reproduce a constant and unidirectional heat flow between the two plates. Although the plates measure 500 mm x 500 mm, the flow generated by the equipment involves an area of 150 mm x 150 mm in the centre. The frame around this measurement area is made of insulating material. Regardless of the insulation conferred by the boundaries of the plates, the specimens were also insulated with an expanded polystyrene (EPS) frame to guarantee the direction of the heat flow and to eliminate lateral heat transfer. the thermal conductivity tests were performed for an average temperature of 10 ºC and a difference of 15 ºC between plates.